



## OPEN ACCESS

## EDITED BY

Jing Zhang,  
University of Toyama, Japan

## REVIEWED BY

Wei Xie,  
Sun Yat-sen University, China  
Duntao Shu,  
Northwest A&F University, China

## \*CORRESPONDENCE

Guodong Song  
gsong@ouc.edu.cn

## SPECIALTY SECTION

This article was submitted to  
Marine Biogeochemistry,  
a section of the journal  
Frontiers in Marine Science

RECEIVED 19 July 2022

ACCEPTED 01 September 2022

PUBLISHED 23 September 2022

## CITATION

Xu H, Song G, Yang S, Zhu R, Zhang G  
and Liu S (2022) Benthic nitrogen  
cycling in the deep ocean of the  
Kuroshio Extension region.  
*Front. Mar. Sci.* 9:997810.  
doi: 10.3389/fmars.2022.997810

## COPYRIGHT

© 2022 Xu, Song, Yang, Zhu, Zhang and  
Liu. This is an open-access article  
distributed under the terms of the  
[Creative Commons Attribution License  
\(CC BY\)](https://creativecommons.org/licenses/by/4.0/). The use, distribution or  
reproduction in other forums is  
permitted, provided the original  
author(s) and the copyright owner(s)  
are credited and that the original  
publication in this journal is cited, in  
accordance with accepted academic  
practice. No use, distribution or  
reproduction is permitted which does  
not comply with these terms.

# Benthic nitrogen cycling in the deep ocean of the Kuroshio Extension region

Haoming Xu<sup>1,2,3</sup>, Guodong Song<sup>1,2\*</sup>, Siqi Yang<sup>1,2,3</sup>,  
Ruosi Zhu<sup>1,2,3</sup>, Guiling Zhang<sup>1,2</sup> and Sumei Liu<sup>1,2</sup>

<sup>1</sup>Frontiers Science Center for Deep Ocean Multispheres and Earth System and Key Laboratory of Marine Chemistry Theory and Technology, Ministry of Education, Ocean University of China, Qingdao, China, <sup>2</sup>Laboratory for Marine Ecology and Environmental Science, Qingdao National Laboratory for Marine Science and Technology, Qingdao, China, <sup>3</sup>College of Chemistry and Chemical Engineering, Ocean University of China, Qingdao, China

Benthic nitrogen cycling, including nitrification, N-loss, and other nitrogen transformations, plays a crucial role in the marine nitrogen budget. However, studies on benthic nitrogen cycling mainly focus on marginal seas, while attention to the deep ocean, which occupies the largest area of the seafloor, is severely lacking. In this study, we investigate the benthic nitrogen cycling in the Kuroshio Extension region (KE) of the northwest Pacific Ocean at water depths greater than 5,000 m through <sup>15</sup>N enrichment slurry incubation and pore-water dissolved oxygen and inorganic nitrogen profiles. The slurry incubation indicates nitrification is the predominant process in benthic nitrogen cycling. The potential nitrification rates are nearly an order of magnitude higher than dissimilatory nitrate reduction. Nitrification and total N-loss flux estimated from pore-water nitrate and ammonium profiles are 6–42 and 5–30  $\mu\text{mol N m}^{-2} \text{d}^{-1}$ , respectively. Generally, anammox is the predominant N-loss process in KE sediment. The temperature gradient experiment indicates that the optimum temperature for anammox and denitrification is 13 and 41°C, respectively, partially explaining anammox as the dominant process for deep-ocean benthic N-loss. Both the low concentration of ammonium in pore-water and the discrepant results between anoxic incubation amended with <sup>15</sup>NO<sub>3</sub><sup>-</sup> and <sup>15</sup>NH<sub>4</sub><sup>+</sup>+<sup>14</sup>NO<sub>3</sub><sup>-</sup> suggest that ammonium is another limiting factor for benthic anammox. N-loss activity gradually declines with the distance from the Oyashio–Kuroshio transition zone. However, nitrification has the opposite trend roughly. This reveals that the sediment in KE transfers from nitrate sink to source from north to south. This trend is mainly caused by the variation of primary production and the supplement of active organic matter, which is the energy source for microbes and the potential source for ammonium through remineralization. Overall, our results highlight temperature and ammonium as two limiting factors for deep-ocean benthic N-loss and also exhibit a tight coupling relationship between pelagic primary production and the benthic nitrogen cycle in KE.

## KEYWORDS

benthic nitrogen cycling, Kuroshio Extension region, abyssal plain, nitrification, denitrification, anammox, DNRA

## Introduction

As an essential element for biological growth, reproduction, and evolution, nitrogen limits the primary production of marine phytoplankton, which regulates global atmospheric CO<sub>2</sub> levels (Howarth and Marino, 2006; Canfield et al., 2010). Therefore, the study of marine nitrogen biogeochemical cycling has always been a hotspot in studies related to global change (Gruber and Galloway, 2008). Marine sediment is the most active zone for nitrogen turnover processes, where more than 50% of fixed nitrogen loss occurs (Devol, 2015). The benthic nitrogen cycle generally includes the mineralization of organic nitrogen, aerobic nitrification, and anaerobic dissimilatory nitrate reduction (Kuypers et al., 2018; Hutchins and Capone, 2022). The primary nitrogen source of marine sediments is the deposition of particulate organic nitrogen. Mineralization then converts burial organic nitrogen into ammonium, supporting other processes (Thamdrup and Dalsgaard, 2008). The removal of nitrogen relies on two dissimilatory nitrate reduction processes: heterotrophic denitrification ( $\text{NO}_3^- \rightarrow \text{NO}_2^- \rightarrow \text{NO} \rightarrow \text{N}_2\text{O} \rightarrow \text{N}_2$ ) and autotrophic anaerobic ammonium oxidation (anammox,  $\text{NH}_4^+ + \text{NO}_2^- \rightarrow \text{N}_2$ ) in the anoxic sediments (Thamdrup and Dalsgaard, 2002), which are collectively known as nitrogen loss processes with a final product of N<sub>2</sub>. Unlike denitrification and anammox, dissimilatory nitrate reduction to ammonium (DNRA,  $\text{NO}_3^- \rightarrow \text{NO}_2^- \rightarrow \text{NH}_4^+$ ) converts nitrate to ammonium, which is retained in the aquatic environment in ion form (Tiedje, 1988). Aerobic nitrification ( $\text{NH}_4^+ \rightarrow \text{NO}_2^- \rightarrow \text{NO}_3^-$ ), including ammonium and nitrite oxidation processes, occurs in the oxic sediment layer and is linked to mineralization and dissimilatory nitrate reduction (Ward, 2008).

The marine benthic nitrogen cycle has been extensively studied in the last decades with the wide application of the <sup>15</sup>N amended incubation experiment and the development of the <sup>15</sup>N analysis technique. However, most of these studies focused on marginal seas, while attention to the deep ocean, which covers about 60% of the seafloor, was relatively scarce. N-loss processes have been studied directly in limited deep continental slope and basin sediments with water depths greater than 1,000 m based on <sup>15</sup>N incubation (Engström et al., 2009; Trimmer and Nicholls, 2009; Sokoll et al., 2012; Na et al., 2018; Rich et al., 2020). Compared with coastal or continental shelf sediment, although the total nitrogen loss rate is relatively low, the psychrophilic and autotrophic anammox processes seem to show a rather substantial contribution to N-loss with increasing water depth (Dalsgaard et al., 2005; Devol, 2015). Thamdrup et al. (2021) first investigated the benthic N-loss in two hadal trenches, Atacama and Kermadec, with water depths of 7,720–7,915 and 9,300–9,555 m, respectively, which is currently the N-loss result with the greatest water depth reported in the marine sediment. Despite being the deepest part of the ocean, hadal trenches receive both vertical and lateral inputs of

organic matter and are believed to be the hotspots for benthic early diagenesis and N-loss processes in deep marine environments (Glud et al., 2021; Thamdrup et al., 2021).

Unlike continental shelves and slopes with relatively shallower overlying water or hadal trenches with abundant organic matter accumulation, in abyssal plain sediment, O<sub>2</sub> is thought to be the significant electron acceptor according to the model results because of the low organic matter deposition. Hence, aerobic nitrification is the predominant nitrogen transformation process (Middelburg et al., 1996; Soetaert et al., 1996). The nitrification and N-loss rates were estimated based on pore-water dissolved inorganic nitrogen (DIN), the natural <sup>15</sup>N abundance profiles, and benthic DIN fluxes supported the viewpoint above as well (Christensen and Rowe, 1984; Brunnegård et al., 2004; Wankel et al., 2015). Nevertheless, few direct measurements of N cycling processes in abyssal plain sediment using <sup>15</sup>N amended incubation have been reported. Therefore, the benthic N cycling behavior and the controlling environmental factors in abyssal plain areas are still unclear.

The Kuroshio Extension region (KE) is located in the North-West of the Pacific Ocean. The submarine topography of KE is mainly an abyssal plain referred to as the Northwest Pacific Basin (Jamieson and Stewart, 2021), which provides an appropriate field for studying benthic nitrogen cycling behavior in the abyssal plain area. In this study, we measured the pore-water dissolved inorganic nitrogen (DIN) profiles and estimated the total rates of nitrification and N-loss. Potential nitrification, anammox, denitrification, and DNRA rates were obtained through oxic and anoxic <sup>15</sup>N amended slurry incubation under *in situ* conditions. Additionally, a temperature gradient anoxic <sup>15</sup>N incubation was conducted to investigate the temperature response of denitrification, anammox, and DNRA in the deep ocean. This study provides the first direct measurement of nitrification, denitrification, anammox, and DNRA in KE sediment, and further explores the benthic nitrogen cycling behavior and the environmental factors regulating these processes in abyssal plain areas.

## Materials and methods

### Station description and sampling procedures

Sampling stations are located in the abyssal plain area of KE (146°12'–151°12' E, 32°24'–41°00' N) with water depths of 5,408–6,011 m (Figure 1 and Table 1). Intense eddy activity and complex currents, which affect nutrient transport, make the pelagic net primary production (NPP) highly variable (Uchiyama et al., 2017; Clayton et al., 2021) and generally decrease from north to south with the distance from the Oyashio–Kuroshio transition region (Figure 1 and Table 1).

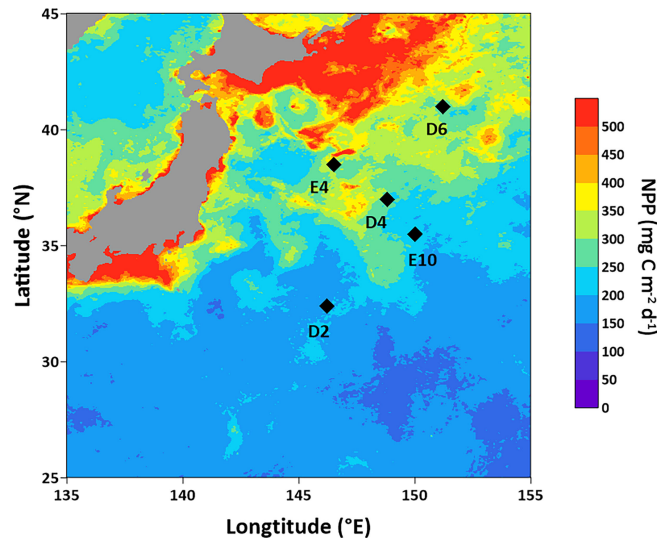


FIGURE 1 Sampling stations in KE. The NPP distribution is based on the online data of Copernicus Marine Environment Monitoring Service (CMEMS, <https://marine.copernicus.eu/>).

Sampling and onboard incubation experiments were conducted during the cruise in May and June 2021 by *R/V Dongfanghong 3*. Sediment was successfully collected using a box corer at five stations (D2, D4, D6, E4, and E10), with visually clear overlying water and an undisturbed sediment surface. Sub-cores were obtained using polycarbonate tubes (length = 30 cm, i. d. = 9.5 cm), sealed with silica gel stoppers. Sediment cores were then transferred to a temperature-controlled incubator and preserved temporarily under the *in situ* temperature for O<sub>2</sub> profile measurement, pore-water sampling, and layered <sup>15</sup>N slurry incubation afterward. At Sta. D6, extra surface sediment (about 0–5 cm) was collected for a temperature gradient <sup>15</sup>N incubation. A portion of segmented sediment for <sup>15</sup>N slurry incubation was collected in zip-lock PE bags and stored at –20°C, subsequently freeze-dried for determination of sediment porosity, total organic carbon (TOC), total nitrogen (TN), and chlorophyll *a* (Chl-*a*) contents.

Sediment O<sub>2</sub> profiles were determined in duplicate or triplicate at each station within 2 h after sampling using an oxygen microelectrode (OX-25, Unisense, Denmark) installed on a micromanipulator with a resolution of 200 μm. Sub-cores for pore-water extraction were segmented immediately every 0.5 or 1 cm in the upper 10 cm and 1 cm in the remaining section. Pore-water was extracted using Rhizon samplers as described by Song et al. (2013) and preserved in 15 ml centrifuge tubes under –20°C for DIN (including NO<sub>3</sub><sup>–</sup>, NO<sub>2</sub><sup>–</sup>, and NH<sub>4</sub><sup>+</sup>) analysis. Bottom water was collected from about 20–50 m above the seafloor, using Niskin bottles coupled to a Conductivity–Temperature–Depth sensor (CTD)-rosette system at each station, except for E10, where the cast was only down to 1,000 m. Water temperature and salinity were simultaneously measured by CTD. The bottom water for DIN analysis was filtered using 0.7 μm GF/F membranes and stored in polyethylene bottles at –20°C.

TABLE 1 Water depth, positions, bottom water temperature, salinity, NO<sub>3</sub><sup>–</sup> and NH<sub>4</sub><sup>+</sup> concentration, and pelagic net primary production (NPP) at each sampling station.

Station	Water depth (m)	Latitude (N)	Longitude (E)	Temperature (°C)	salinity	NO <sub>3</sub> <sup>–</sup> (μmol L <sup>–1</sup> )	NH <sub>4</sub> <sup>+</sup> (nmol L <sup>–1</sup> )	NPP (mg C m <sup>–2</sup> d <sup>–1</sup> )
D2	5894	32°24′	146°12′	1.60	34.69	36.38	14	185.3
D4	5826	37°00′	148°48′	1.60	34.69	36.24	12	251.3
D6	5548	41°00′	151°12′	1.59	34.69	36.34	15	287.6
E4	5408	38°30′	146°30′	1.54	34.69	36.74	15	313.7
E10	6011	35°30′	150°00′	/	/	/	/	216.9

Temperature and salinity were measured using a CTD probe. NPP derived from the monthly remote sensing data (01.09.1997–01.06.2021) was provided by Copernicus Marine Environment Monitoring Service (CMEMS, <https://marine.copernicus.eu/>).

## <sup>15</sup>N slurry incubation under *in situ* temperature

Both oxic and anoxic <sup>15</sup>N enrichment slurry incubations under *in situ* temperature were carried out to determine the potential rates of nitrification and dissimilatory nitrate reduction processes (including denitrification, anammox, and DNRA), respectively. We chose the bag incubation style (Hansen et al., 2000), and the operating procedure of the slurry incubation referred to by Thamdrup and Dalsgaard (2002) and Song et al. (2013) with slight modifications as described below. The division of oxic and anoxic incubation was conducted according to the O<sub>2</sub> profile at each station. For Sta. D2, a pore-water O<sub>2</sub> profile under 6 cm was not obtained (see Results). Thus, 17–19 and 19–21 cm of sediment were predicted to be anoxic and were used for anoxic <sup>15</sup>N enrichment slurry incubation.

For oxic incubation, 20 ml of homogenized sediment and 180 ml of air-flushed bottom water were mixed in a gas-tight bag. The artificial seawater described below was used for Sta. E10. Each bag was amended with <sup>15</sup>NH<sub>4</sub><sup>+</sup> or <sup>15</sup>NO<sub>2</sub><sup>-</sup> with the final <sup>15</sup>N tracer concentration of about 100 μmol L<sup>-1</sup>. The slurry was sub-sampled from the incubation bag at five time-points within 72 h at Sta. D2 and 48 h at Sta. D4, D6, E4, and E10, respectively. The sub-samples were preserved in 5.9 ml vials (Labco, United Kingdom) pre-filled with 0.1 ml of saturated HgCl<sub>2</sub> solution for the determination of <sup>15</sup>NO<sub>X</sub><sup>-</sup> (<sup>15</sup>NO<sub>3</sub><sup>-</sup> and <sup>15</sup>NO<sub>2</sub><sup>-</sup>). Dissolved oxygen in the slurry was determined by the O<sub>2</sub> microelectrode mentioned above before the Exetainer bottle cap was tightened to ensure the oxic conditions during the incubation process.

For anoxic incubation, 20 ml of homogenized sediment and 180 ml of He-flushed artificial seawater (35 g NaCl and 0.2 g NaHCO<sub>3</sub> in 1 L of purified water, with a nitrate background less than 3 μmol L<sup>-1</sup>) were mixed in a gas-tight bag. The slurry was preincubated under *in situ* conditions for 2–4 days to remove the residual O<sub>2</sub>. The anoxic condition in the incubation bag was confirmed by the O<sub>2</sub> microelectrode described above. After the preincubation, each bag was amended with He-flushed <sup>15</sup>NO<sub>3</sub><sup>-</sup> or <sup>15</sup>NH<sub>4</sub><sup>+</sup> + <sup>14</sup>NO<sub>3</sub><sup>-</sup> stock solution with a final <sup>15</sup>N tracer concentration of about 100 μmol L<sup>-1</sup>. The slurry was sub-sampled from the incubation bag at five time-points within 96 h at Sta. D2 and 48 h at Sta. D4, D6, E4, and E10, respectively. The preservation of the samples was the same as for the aerobic incubation. Nevertheless, the target parameters for the assay were <sup>15</sup>N<sub>2</sub> (<sup>29</sup>N<sub>2</sub> and <sup>30</sup>N<sub>2</sub>) and <sup>15</sup>NH<sub>4</sub><sup>+</sup> instead of <sup>15</sup>NO<sub>X</sub><sup>-</sup>. For DIN analysis, a portion of each sub-sample was filtered using a 0.2 μm syringe filter and stored at -20°C.

## Temperature gradient experiment

To investigate the temperature response of dissimilatory nitrate reduction processes in deep-ocean sediment, a temperature gradient anoxic <sup>15</sup>N slurry incubation was

conducted using the upper 5 cm of sediment at Sta. D6. The incubation and sub-sampling procedures were the same as described above but under 16 different temperature gradients (1, 2, 4, 7, 10, 13, 16, 19, 22, 25, 29, 33, 37, 41, 45, 49 °C) in individual temperature-controlling incubators. The optimal temperature at which denitrification or anammox had the highest potential rate was thought to be the optimal temperature (T<sub>opt</sub>). The obvious activation energy (E<sub>a</sub>) was calculated using the Arrhenius equation according to Dalsgaard and Thamdrup (2002).

## Analytical methods

The isotopic ratios of <sup>29</sup>N<sub>2</sub>/<sup>28</sup>N<sub>2</sub> and <sup>30</sup>N<sub>2</sub>/<sup>28</sup>N<sub>2</sub> were determined using a homemade membrane-inlet mass spectrometer (MIMS) according to Kana et al. (1994). The typical precision of the <sup>29</sup>N<sub>2</sub>/<sup>28</sup>N<sub>2</sub> and <sup>30</sup>N<sub>2</sub>/<sup>28</sup>N<sub>2</sub> determinations is 0.1% and 1%, respectively. Concentrations of <sup>29</sup>N<sub>2</sub> and <sup>30</sup>N<sub>2</sub> were calculated according to Thamdrup and Dalsgaard (2000). The linear calibration factor α was determined by the standard working solution, which was made using the same salinity of seawater collected in the investigated region at 20 ± 0.01°C using the air equilibrium method (Kana et al., 1994). The concentration of <sup>15</sup>NH<sub>4</sub><sup>+</sup> was determined using a hypobromite oxidation MIMS method (Yin et al., 2014). <sup>15</sup>NO<sub>2</sub><sup>-</sup> was first converted to <sup>29</sup>N<sub>2</sub> by the sulfamic acid reduction method (Granger and Sigman, 2009), then its concentration was determined by the same MIMS described above. <sup>15</sup>NO<sub>X</sub><sup>-</sup> was reduced to <sup>15</sup>NO<sub>2</sub><sup>-</sup> by the vanadium trichloride method (Schnetger and Lehnert, 2014), then its concentration was determined as <sup>15</sup>NO<sub>2</sub><sup>-</sup> described above. The concentration of <sup>15</sup>NO<sub>3</sub><sup>-</sup> was calculated from the difference between <sup>15</sup>NO<sub>X</sub><sup>-</sup> and <sup>15</sup>NO<sub>2</sub><sup>-</sup>. The DIN of bottom water, pore-water, and incubation samples was determined by the spectrophotometric method using a nutrient auto-analyzer (AA3, SEAL, United Kingdom), except for the bottom water NH<sub>4</sub><sup>+</sup> concentration, which was determined by a high-sensitivity fluorescence method (Holmes et al., 1999).

Sediment porosity was calculated from the difference between the wet and dry weight of the sediment, considering the dry sediment density of 2.65 g cm<sup>-3</sup> and the seawater density of 1.02 g cm<sup>-3</sup>. Sediment TOC and TN content were determined using an elemental analyzer (Vario EL III, Elementar, Germany). The precision for TOC and TN determination is 5% (standard sample TOC = 0.56%) and 2% (standard sample TN = 0.06%), respectively. Sediment Chl-*a* was determined in triplicate using a fluorometric method (Pinckney et al., 1994).

## Rate calculations

Benthic O<sub>2</sub> and DIN fluxes from profiles were calculated using Fick's first law of diffusion from the steady state assuming a section with linear O<sub>2</sub> and DIN concentration gradient

through Equation (1) (Brunnegård et al., 2004; Engström et al., 2009):

$$F_{sed} = -\varnothing D_{sed} \frac{dc}{dz} \quad (1)$$

where  $F_{sed}$  is the flux in sediment,  $\varnothing$  is the porosity of the sediment,  $dc/dz$  is the linear concentration gradient in sediment pore-water;  $D_{sed}$  is the diffusion coefficient in sediment and is calculated by Equation (2) according to Boudreau (1997):

$$D_{sed} = \frac{D_{sw}}{1 - \ln(\varnothing^2)} \quad (2)$$

where  $D_{sw}$  is the diffusion coefficient in seawater, obtained by Li and Gregory (1974).

Total nitrification and N-loss rates were estimated from DIN fluxes in sediment (Brunnegård et al., 2004; Engström et al., 2009; Thamdrup et al., 2021). DIN fluxes in the sediment oxic zone (OZ) and anoxic nitrogenous zone (NZ) were calculated separately. The estimations were based on the following assumptions: (1) Nitrate from nitrification supplied the N-loss processes and diffused to the overlying water meanwhile; (2) Downward nitrate flux in NZ was used for N-loss through denitrification and anammox; (3) Upward ammonium flux in NZ was used for anammox. Thus, rates of nitrification, denitrification, anammox, and total N-loss were calculated using Equations (3–6):

$$N_F = -F_{NO_3^-}(OZ) + F_{NO_3^-}(NZ) \quad (3)$$

$$D_F = F_{NO_3^-}(NZ) + F_{NH_4^+}(NZ) \quad (4)$$

$$A_F = -2F_{NH_4^+}(NZ) \quad (5)$$

$$NL_F = D_F + A_F \quad (6)$$

where  $N_F$ ,  $D_F$ ,  $A_F$ , and  $NL_F$  were the total rate of nitrification, denitrification, anammox, and N-loss from DIN fluxes, respectively;  $F_{NO_3^-}$  (OZ),  $F_{NO_3^-}$  (NZ) and  $F_{NH_4^+}$  (NZ) represents nitrate or ammonium flux in the sediment oxic zone or the anoxic nitrogenous zone.

The potential rates of nitrification, denitrification, anammox, and DNRA were calculated from  $^{15}N$  slurry incubation using the isotope pairing technique (IPT). Equations according to Thamdrup and Dalsgaard (2002) were used in this study without considering the minor influence of DNRA on anammox. Therefore, the potential rates were calculated using Equations (7–12):

$$N_{P1} = \frac{P_{^{15}NO_x^-}}{F_A} \quad (7)$$

$$N_{P2} = \frac{P_{^{15}NO_3^-}}{F_{NI}} \quad (8)$$

$$D_P = \frac{P_{30}}{F_N^2} \quad (9)$$

$$A_{P1} = \frac{P_{29} - 2 \times \left(\frac{1}{F_N} - 1\right) \times P_{30}}{F_N} \quad (10)$$

$$A_{P2} = \frac{P_{29}}{F_A} \quad (11)$$

$$DNRA_P = \frac{P_{^{15}NH_4^+}}{F_N} \quad (12)$$

where  $N_{P1}$  and  $N_{P2}$  were the potential nitrification rate from  $^{15}NH_4^+$  and  $^{15}NO_3^-$  amended incubation, respectively;  $D_P$  was the potential denitrification rate from  $^{15}NO_3^-$  amended incubation;  $A_{P1}$  and  $A_{P2}$  were the potential anammox rates from  $^{15}NO_3^-$  and  $^{15}NH_4^+ + ^{14}NO_3^-$  amended incubation, respectively;  $DNRA_P$  was the potential DNRA rate from  $^{15}NO_3^-$  amended incubation;  $P_{29}$ ,  $P_{30}$ ,  $P_{^{15}NO_x^-}$ ,  $P_{^{15}NO_3^-}$ , and  $P_{^{15}NH_4^+}$  were the production rates of  $^{29}N_2$ ,  $^{30}N_2$ ,  $^{15}NO_x^-$ ,  $^{15}NO_3^-$ , and  $^{15}NH_4^+$ , respectively;  $F_A$ ,  $F_{NI}$ , and  $F_N$  were the  $^{15}N$  abundance of ammonium, nitrite, and nitrate in the  $^{15}N$  enrichment incubation, respectively.

The relative contribution of anammox to N-loss was calculated using Equation (13):

$$ra = \frac{A}{A + D} \times 100\% \quad (13)$$

where A and D were the anammox and denitrification rates, respectively, including potential rates ( $A_P$  and  $D_P$ ) and rates estimated from DIN fluxes ( $A_F$  and  $D_F$ ).

## Statistical analysis

The significance of  $^{15}N_2$  and  $^{15}NO_x^-$  production in  $^{15}N$  slurry incubation was tested by linear regression between the  $^{15}N$  concentration and time, with a critical p-value of 0.05. Correlations between potential nitrification or anammox rates and environmental factors (TOC, TN, and Chl-*a*) were conducted by Pearson correlation with a critical p-value of 0.10. Correlations between total nitrification or  $NO_3^-$  loss rates and water depth or pelagic net primary production (NPP) were conducted by Pearson correlation with a critical p-value of 0.05. All statistical analyses were run using the Sigmaplot software.

## Results

### Bottom water and sediment characteristics

Bottom water characteristics at all stations are shown in Table 1, except Sta. E10, where the bottom water was not



sampled at that time. The bottom water temperature and salinity were all about 2°C and 35 during the cruise, respectively. The nitrate and ammonium concentrations of bottom water at each station varied little (36.24–36.74  $\mu\text{mol L}^{-1}$  and 12–15  $\text{nmol L}^{-1}$  for nitrate and ammonium, respectively). Four sediment cores from Sta. D2, D4, D6, E10, and surface and bottom sediment from Sta. E4 in the KE were obtained and characterized. The general characteristics of the investigated sediments are shown in Table 2. The porosity of the sediment had an average value of  $0.80 \pm 0.06$  and declined with depth generally. Sediment TOC, TN, and Chl-*a* content were 0.28%–0.80%, 0.11%–0.19%, and 0.03–2.02  $\mu\text{g g}^{-1}$ , respectively. All generally decreased vertically with sediment depth. Sediment at northern Sta. E4 had the highest organic matter content (TOC = 0.80%; TN = 0.18%; Chl-*a* =  $2.02 \pm 0.07 \mu\text{g g}^{-1}$ ) and sediment at southern Sta. D2 had the lowest (TOC = 0.28%; TN = 0.11%;  $0.03 \pm 0.00 \mu\text{g g}^{-1}$ ). Though the bottom water at different stations varied little, the characteristics of sediments showed a significant discrepancy from north to south in KE.

## Pore-water $\text{O}_2$ and dissolved inorganic nitrogen distribution

Pore-water  $\text{O}_2$  generally decreases with depth and eventually depletes (except at Sta. D2). The penetration depths of  $\text{O}_2$  at Sta. D4, D6, and E10 were 15, 20, and 50 mm, respectively. While at Sta. D2, the  $\text{O}_2$  concentration in pore-water can still come up to about 100  $\mu\text{mol L}^{-1}$  at a depth of 60 mm, the maximum

measurement depth for our  $\text{O}_2$  electrode, and the  $\text{O}_2$  penetration depth at Sta. D2 was supposed to be far more than 100 mm (Figure 2A). Benthic  $\text{O}_2$  consumption flux ranged between 867 and 2,017  $\mu\text{mol O}_2 \text{ m}^{-2} \text{ d}^{-1}$  (Table 3) and was highest at the northern station D6, with high pelagic NPP and sediment TOC content. Generally, the penetration depth of  $\text{O}_2$  gradually increased from north to south in KE, revealing a decrease in benthic  $\text{O}_2$  consumption as well.

The nitrate profiles in sediment pore-water showed distinctly different patterns from south to north at different stations (Figure 2B). For Sta. D2, the southernmost station, nitrate accumulated downward; no consumption was observed for the whole sediment core obtained was oxic; for Sta. D4 and E10, nitrate accumulated in the oxic zone (0–1 cm and 0–5 cm for D4 and E10, respectively) and started to accumulate in the lower anoxic zone. Nitrate was depleted at 15 cm for Sta. D4 still existed at 25 cm with a concentration near 30  $\mu\text{mol L}^{-1}$  for Sta. E10; for Sta. D6, nitrate was consumed at the beginning and was depleted at 5 cm. Nitrate accumulation at surface sediment was not detected in Sta. D6 for the high-N-loss rates, similar to coastal and shelf sediments. Limited by the sediment sampling method (box corer), we could hardly obtain sediment samples under 30 cm. It might be possible to observe nitrate consumption and even depletion in the deeper layer at stations with low-N-loss activities like Sta. D2 and E10, using a gravity corer. Generally, pore-water nitrate first accumulates in the oxic layer and is then consumed in the anoxic layer. However, the nitrate accumulation layer was relatively thicker in southern KE with lower pelagic primary production.

TABLE 2 General characteristics of investigated sediments.

Station	Sediment depth (cm)	Porosity	TOC (% dry wt)	TN (% dry wt)	C: N	Chl- <i>a</i> ( $\mu\text{g g}^{-1}$ dry wt)
D2	0–1	0.84	0.56	0.11	5.3	$0.93 \pm 0.05$
	1–3	0.76	0.44	0.10	4.3	$0.17 \pm 0.01$
	3–5	0.72	0.40	0.09	4.4	$0.13 \pm 0.02$
	5–7	0.74	0.41	0.11	3.9	$0.09 \pm 0.01$
	17–19	0.64	0.28	0.11	2.6	$0.03 \pm 0.00$
	19–21	0.73	0.28	0.11	2.6	$0.03 \pm 0.00$
D4	~0–3*	0.85	0.71	0.17	4.0	$0.74 \pm 0.02$
	~6–9*	0.73	0.75	0.16	4.6	$1.29 \pm 0.01$
D6	0–1	0.87	0.69	0.18	3.9	$1.58 \pm 0.02$
	1–3	0.86	0.68	0.13	5.1	$1.58 \pm 0.03$
	3–5	0.86	0.66	0.15	4.5	$1.48 \pm 0.01$
	5–7	0.86	0.64	0.17	3.8	$1.45 \pm 0.01$
	7–9	0.83	0.60	0.16	3.7	$1.33 \pm 0.02$
E4	9–11	0.80	0.61	0.15	4.0	$1.38 \pm 0.04$
	~0–3*	0.83	0.77	0.19	4.0	$1.04 \pm 0.01$
	~6–9*	0.83	0.80	0.18	4.5	$2.02 \pm 0.07$
E10	~0–3*	0.80	0.53	0.15	3.6	$0.21 \pm 0.01$
	~6–9*	0.78	0.43	0.13	3.2	$0.13 \pm 0.00$

\*Sediments were directly dug from the surface and the bottom of the box corer. The sampling depth was approximately 0–3 and 6–9 cm, respectively.

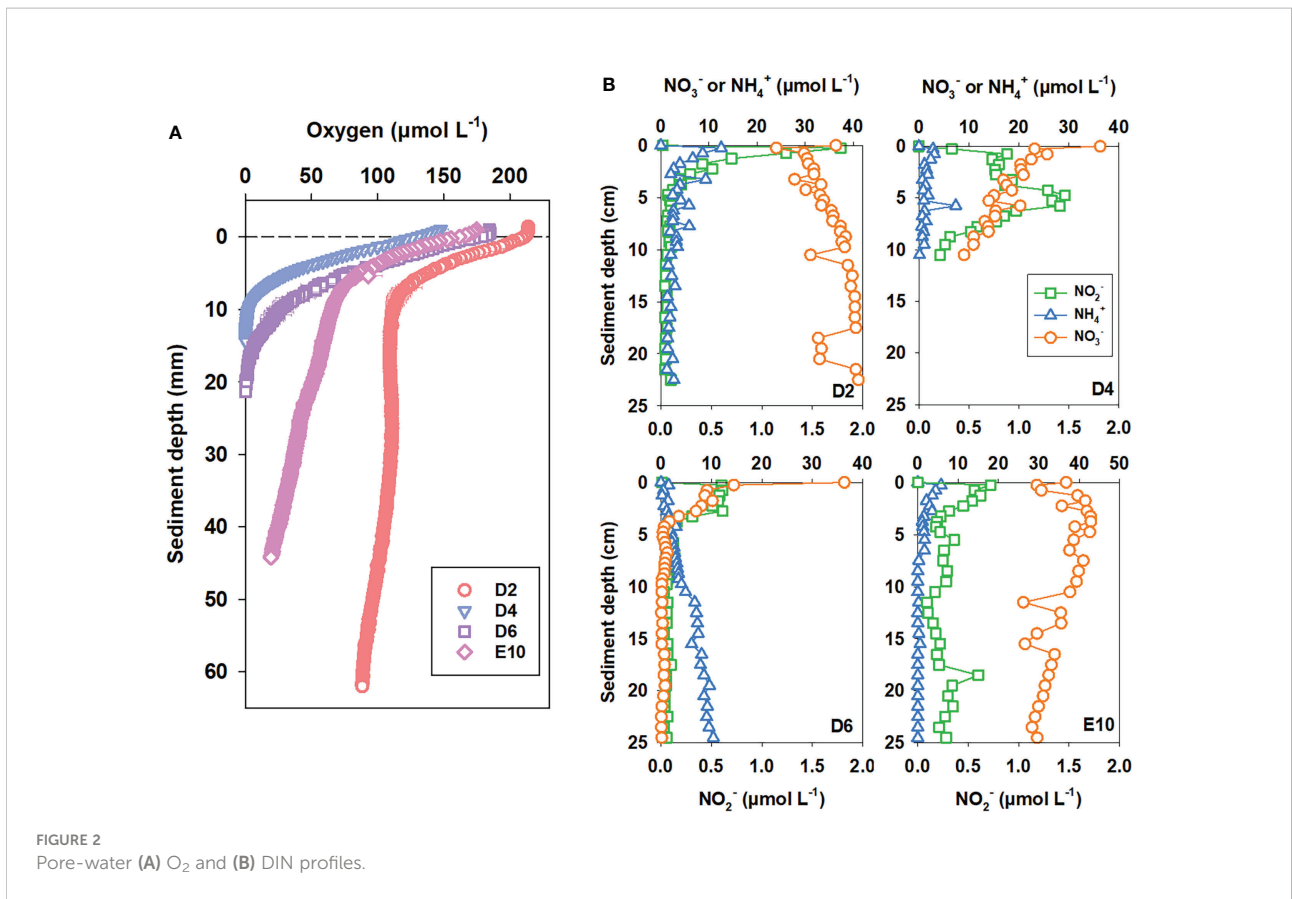


FIGURE 2 Pore-water (A) O<sub>2</sub> and (B) DIN profiles.

Unlike the profiles of ammonium in sediment pore-water on the continental shelf of the marginal seas, the profiles of ammonium in sediment pore-water at all three stations on this cruise, except at station D6, showed extreme values in the surface layer (Figure 2B). This result is similar to previous studies in the deep ocean and is likely due to artifacts during the sampling and transportation processes (Hall et al., 2007; Engström et al., 2009).

As the sediment depth increased, the concentration of ammonium in the pore-water gradually decreased until it could no longer be detected at the respective depths (Figure 2B). At Sta. D6, the concentration of ammonium in the pore-water showed accumulation with increased sediment depth (Figure 2B). Pore-water ammonium concentrations are maintained at a lower level in KE but higher at northern stations.

TABLE 3 O<sub>2</sub> fluxes (μmol O<sub>2</sub> m<sup>-2</sup> d<sup>-1</sup>) and DIN fluxes (μmol N m<sup>-2</sup> d<sup>-1</sup>) estimated from pore-water profiles and rates of benthic N cycle processes (μmol N m<sup>-2</sup> d<sup>-1</sup>) of each station estimated from DIN fluxes (OZ, oxic zone; NZ, anoxic nitrogenous zone).

Station	D2	D4	D6	E10
O <sub>2</sub> flux	867 ± 20	1,472 ± 55	2,017 ± 99	1,375 ± 71
NO <sub>3</sub> <sup>-</sup> flux (OZ)	-6 ± 1	-29	5	-14 ± 5
NO <sub>3</sub> <sup>-</sup> flux (NZ)	/	13 ± 2	22 ± 2	4 ± 0
NH <sub>4</sub> <sup>+</sup> flux (NZ)	/	/	-8 ± 1	/
Nitrification (N <sub>P</sub> )	>6 ± 1	42 ± 2	17 ± 2	18 ± 5
Nitrification (N <sub>IP</sub> )	290 ± 25	147 ± 14	21 ± 19	231 ± 56
Total N loss	/	~17–26*	30 ± 2	~5–8*
Denitrification	/	/	14 ± 2	/
Anammox	/	/	16 ± 2	/
ra (%)	/	/	52.8 ± 7.5	/

\*Rates of total N loss estimated from NO<sub>3</sub><sup>-</sup> flux predicting ra = 50%–100%. Integrated potential nitrification rates (N<sub>IP</sub>) from <sup>15</sup>N incubation in the oxic sediment zone are also displayed here for comparison. The errors are calculated by the standard deviation of the plots relative to the linear regression curve.

## DIN fluxes and nitrogen cycling processes rates estimated from pore-water profiles

The estimated nitrate and ammonium fluxes in the oxic and anoxic zones of the sediment at each station, based on pore-water profiles, are shown in Table 3. Nitrate accumulated downward in the oxic zone at Sta. D2, D4, and E10, with fluxes of  $-6 \pm 1$ ,  $-29$ , and  $-14 \pm 5 \mu\text{mol N m}^{-2} \text{d}^{-1}$ , respectively. For Sta. D6, nitrate was consumed in the oxic zone with a flux of  $5 \mu\text{mol N m}^{-2} \text{d}^{-1}$ . Nitrate consumption fluxes at Sta. D4, D6, and E10 in the anoxic zone were  $13 \pm 2$ ,  $22 \pm 2$ , and  $4 \pm 0 \mu\text{mol N m}^{-2} \text{d}^{-1}$ , respectively. The downward ammonium accumulation in the anoxic zone was observed only at Sta. D6 with a flux of  $-8 \pm 1 \mu\text{mol N m}^{-2} \text{d}^{-1}$ .

Nitrification estimated from DIN fluxes at Sta. D4, D6, and E10 was  $42 \pm 2$ ,  $17 \pm 2$ , and  $18 \pm 5 \mu\text{mol N m}^{-2} \text{d}^{-1}$ , respectively. For Sta. D2, because of unobserved nitrate consumption, nitrification is supposed to be more than  $6 \pm 1 \mu\text{mol N m}^{-2} \text{d}^{-1}$ , the downward nitrate accumulation flux in the oxic zone. Meanwhile, the N-loss rate at Sta. D2 cannot be estimated for the same reason. Sta. D6 is the only station where downward nitrate consumption and ammonium accumulation in anoxic sediment are observed. Thus, denitrification and anammox can be estimated with rates of  $14 \pm 2$  and  $16 \pm 2 \mu\text{mol N m}^{-2} \text{d}^{-1}$ , respectively. The relative contribution of anammox to total N-loss (ra) at Sta. D6 is  $52.8 \pm 7.5\%$ . Due to the relatively higher TOC in sediment at D6, the contribution of anammox as an autotrophic process is supposed to be greater at other stations. Thus, with the prediction of ra of 50%–100%, total N-loss at D4 and E10 is about 17–26 and 5–8  $\mu\text{mol N m}^{-2} \text{d}^{-1}$ , respectively. There is a correlation between total N-loss and pelagic primary production ( $p = 0.084$ , confidence coefficient = 0.90), while the correlation for nitrification is not significant ( $p = 0.407$ ). The N-loss rate estimated from DIN fluxes generally decreases from north to south, while the nitrification rate was relatively higher at the middle station D4.

## Oxic $^{15}\text{N}$ slurry incubation experiments under *in situ* temperature

The linear production of  $^{15}\text{NO}_x^-$  ( $^{15}\text{NO}_2^-$ , and  $^{15}\text{NO}_3^-$ ) over time in both  $^{15}\text{NH}_4^+$  and  $^{15}\text{NO}_2^-$  amended oxic incubations proved the presence of nitrification (including ammonium oxidation and nitrite oxidation) in the oxic sediments of KE (Figures 3A, B). Potential nitrification rates calculated from  $^{15}\text{NO}_2^-$  amended incubations were about 3–18 times higher than  $^{15}\text{NH}_4^+$  amended incubations (Figure 4A). In  $^{15}\text{NH}_4^+$  amended incubation, the  $^{15}\text{NO}_2^-$  production rate was lower than  $^{15}\text{NO}_3^-$  at each station, contributing about 0%–45% (Figure 5, average  $24 \pm 17\%$ ) to total ammonium oxidation.

Potential nitrification rates ( $\text{NH}_4^+$  to  $\text{NO}_3^-$ ) calculated from  $^{15}\text{NH}_4^+$  modified incubations varied between  $1.03 \pm 0.98$  and  $9.81 \pm 0.93 \text{ nmol N cm}^{-3}$  (wet sediment)  $\text{d}^{-1}$ , with neither a significant correlation with TOC, TN nor Chl-*a* (Figures 6A–C,  $p = 0.588$ ,  $0.731$ , and  $0.815$ , respectively). Nitrification activity was highest in near-surface sediment and decreased gradually with depth (Figure 5). Integrated potential nitrification rates from  $^{15}\text{N}$  incubation in the oxic sediment zone generally showed an increasing trend from north to south (Table 3), with the distance from the Kuroshio–Oyashio transition region.

## Anoxic $^{15}\text{N}$ slurry incubation experiments under *in situ* temperature

The linear production of  $^{29}\text{N}_2$  over time in  $^{15}\text{NH}_4^+ + ^{14}\text{NO}_3^-$  amended anoxic incubation at each station (except for Sta. D2 17–19 cm) proved the presence of anammox in the anoxic sediments of KE (Figure 3C, D). However,  $^{30}\text{N}_2$  and  $^{15}\text{NH}_4^+ + ^{15}\text{NH}_4^+$  were not significantly produced in  $^{15}\text{NO}_3^-$  amended incubation at any station, indicating the deficient activity of denitrification and dissimilatory nitrate reduction to ammonium (DNRA) under *in situ* conditions. Potential anammox rates calculated from  $^{15}\text{NH}_4^+ + ^{14}\text{NO}_3^-$  incubations were mainly higher than amended (Figure 4B).

Potential anammox rates calculated from  $^{15}\text{NH}_4^+ + ^{14}\text{NO}_3^-$  ranged from 0 to  $0.31 \pm 0.06 \text{ nmol N cm}^{-3}$  (wet sediment)  $\text{d}^{-1}$  with significant linear correlation with TOC, TN, and Chl-*a* (Figures 6D–F,  $p = 0.012$ ,  $0.003$ , and  $0.088$ , respectively), showing a decreasing trend from north to the south with the distance from the Kuroshio–Oyashio transition region (Figure 5). For Sta. D6, the maximum anammox rate appeared in the 5–7 cm layer where nitrate was depleted and ammonium started to accumulate, while rates in other layers had little difference. Limited by data of layered potential anammox rates and nitrate penetration depth we obtained, we cannot calculate the integrated potential rate of anammox in the sediment anoxic zone at each station.

## Temperature gradient experiment

Potential rates of denitrification and anammox at Sta. D6 increased with temperature at the beginning and started to decrease after the optimal temperature ( $T_{\text{opt}}$ ), which is  $41^\circ\text{C}$  for denitrification and  $13^\circ\text{C}$  for anammox (Figure 7A). The relative contribution of anammox to N-loss (ra) was highest at low temperatures and decreased with temperature to near zero eventually. The potential DNRA rate rose wavelike before  $29^\circ\text{C}$ , and the  $T_{\text{opt}}$  for DNRA is unidentified (Figure 7B). The apparent activation energy ( $E_a$ ) calculated by the Arrhenius equation was  $174.2 \pm 9.6$ ,  $54.5 \pm 10.2$ , and  $91.9 \pm 22.9 \text{ kJ mol}^{-1}$  for denitrification, anammox, and DNRA, respectively. As a



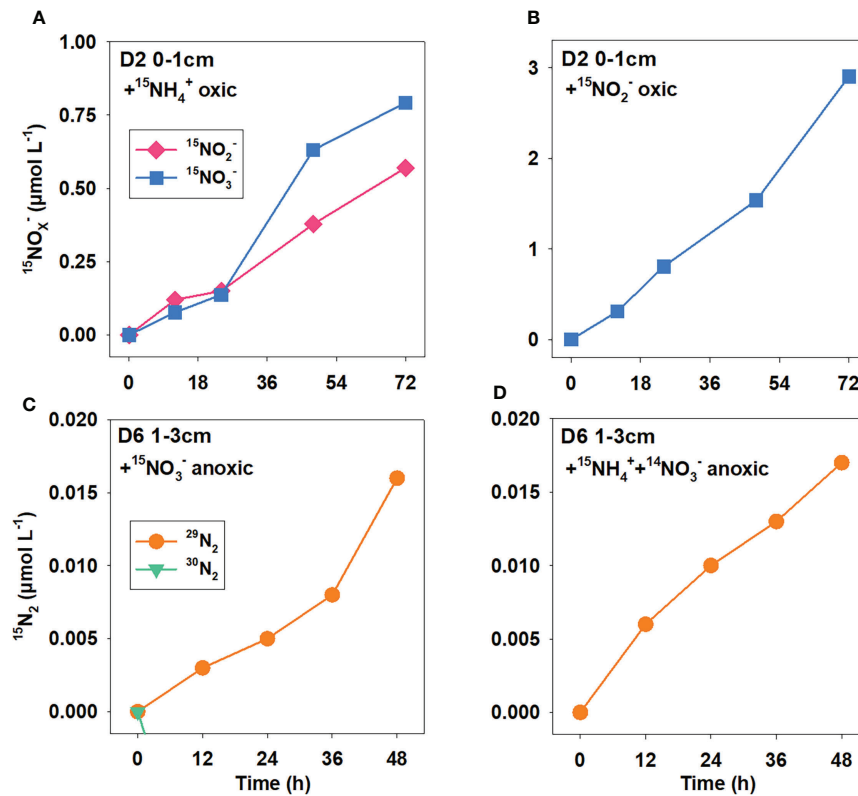


**FIGURE 3** Production of  $^{15}\text{NO}_x^-$  ( $^{15}\text{NO}_3^-$  and  $^{15}\text{NO}_2^-$ ) and  $^{15}\text{N}_2$  ( $^{29}\text{N}_2$  and  $^{30}\text{N}_2$ ) over time in anoxic and oxic  $^{15}\text{N}$  enrichment slurry incubations, respectively. (A) oxic incubation amended with  $^{15}\text{NH}_4^+$ ; (B) oxic incubation amended with  $^{15}\text{NO}_2^-$ ; (C) anoxic incubation amended with  $^{15}\text{NO}_3^-$ ; and (D) anoxic incubation amended with  $^{15}\text{NH}_4^+ + ^{14}\text{NO}_3^-$ .

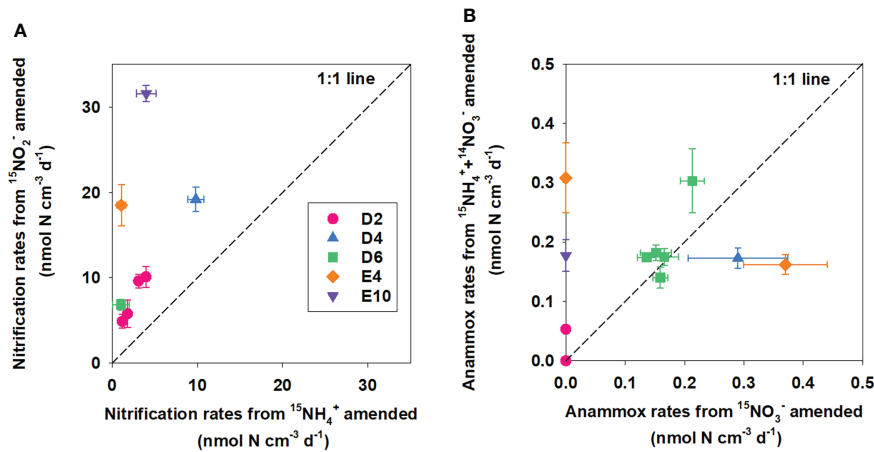


**FIGURE 4** Comparison between (A) potential nitrification rates obtained from oxic incubations amended with  $^{15}\text{NH}_4^+$  and  $^{15}\text{NO}_2^-$ ; (B) potential anammox rates obtained from anoxic incubations amended with  $^{15}\text{NO}_3^-$  and  $^{15}\text{NH}_4^+ + ^{14}\text{NO}_3^-$ .

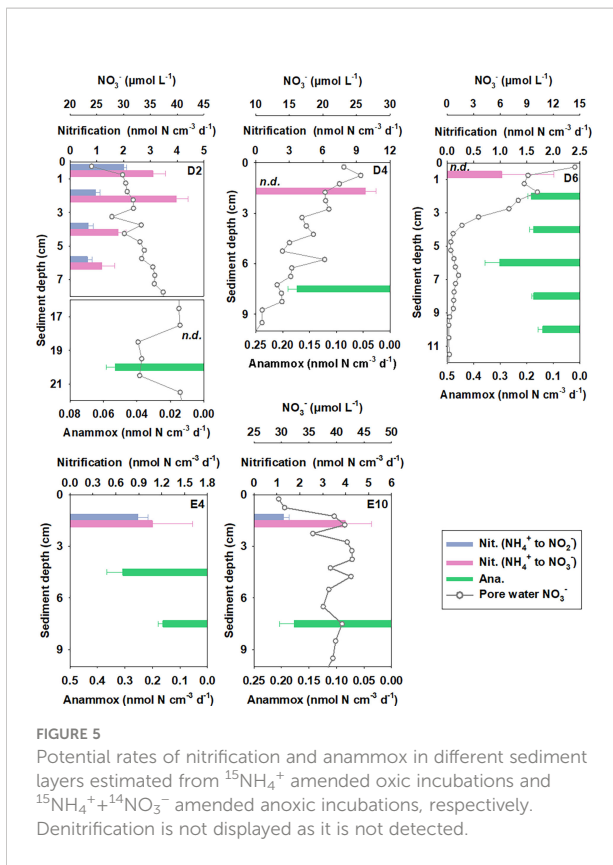


FIGURE 5 Potential rates of nitrification and anammox in different sediment layers estimated from  $^{15}\text{NH}_4^+$  amended oxic incubations and  $^{15}\text{NH}_4^+ + ^{14}\text{NO}_3^-$  amended anoxic incubations, respectively. Denitrification is not displayed as it is not detected.

whole, the temperature response of denitrification, anammox, and DNRA differed sharply in deep-ocean sediment.

## Discussion

### Anammox as a predominant process of N loss in KE sediment

Denitrification and anammox are two major fixed inorganic nitrogen removal pathways in marine sediment. The relative contribution of denitrification and anammox to total nitrogen loss, which affects the nitrogen budget, varies in different marine environments. Therefore, it has gained much attention over the last two decades (Devol, 2015; Chen et al., 2021). However, compared to marginal seas, studies on deep-ocean sediment are still scarce. Previous studies on benthic N-loss in the deep marine environment based on DIN flux and  $^{15}\text{N}$  slurry and intact core incubation (Table 4) all indicate anammox as a significant N-loss process in deep-sea sediment (most ra >40%). In our results, fluxes of denitrification and anammox are in the same order of magnitude compared to previous studies. It seems to be a consensus that the contribution of anammox has a decreasing trend with the increasing TOC content in sediment because denitrification as a heterotrophic process is enhanced (Dalsgaard et al., 2005). On account of the

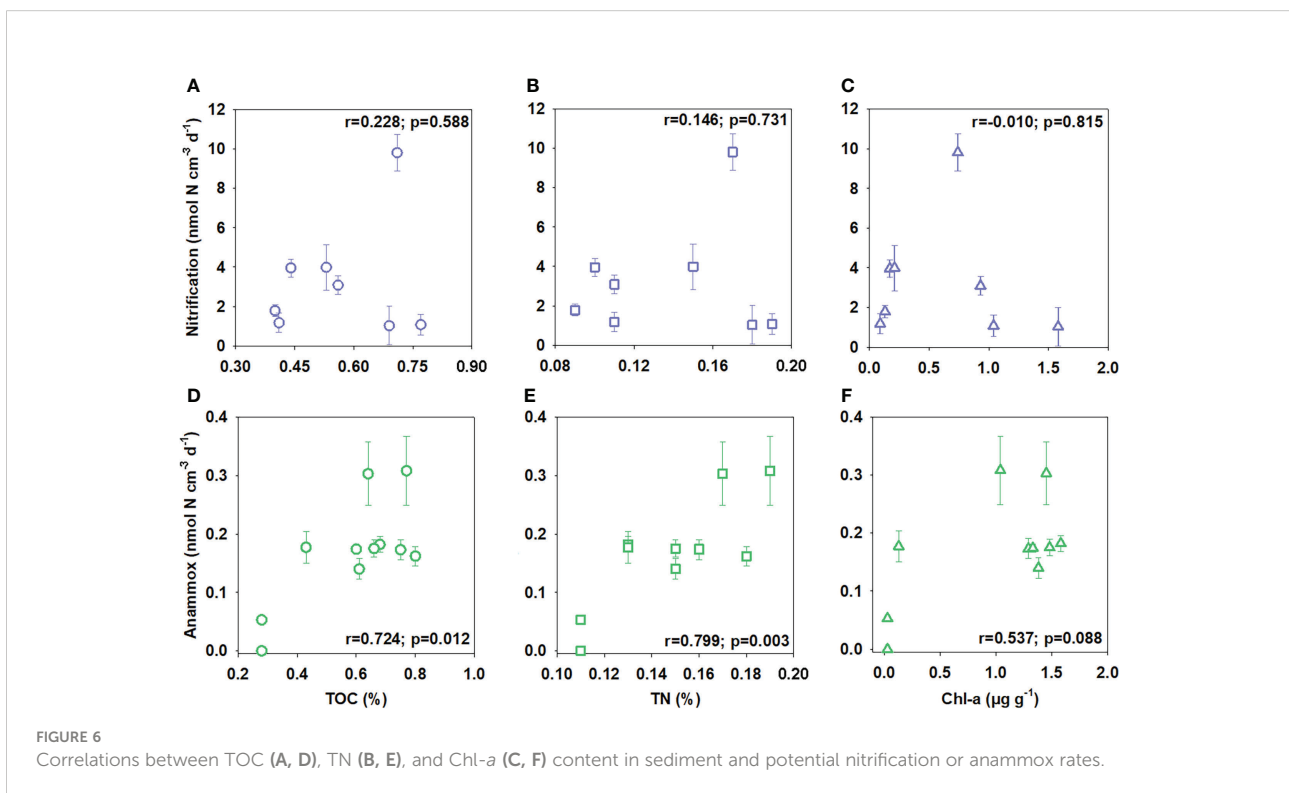


FIGURE 6 Correlations between TOC (A, D), TN (B, E), and Chl-a (C, F) content in sediment and potential nitrification or anammox rates.

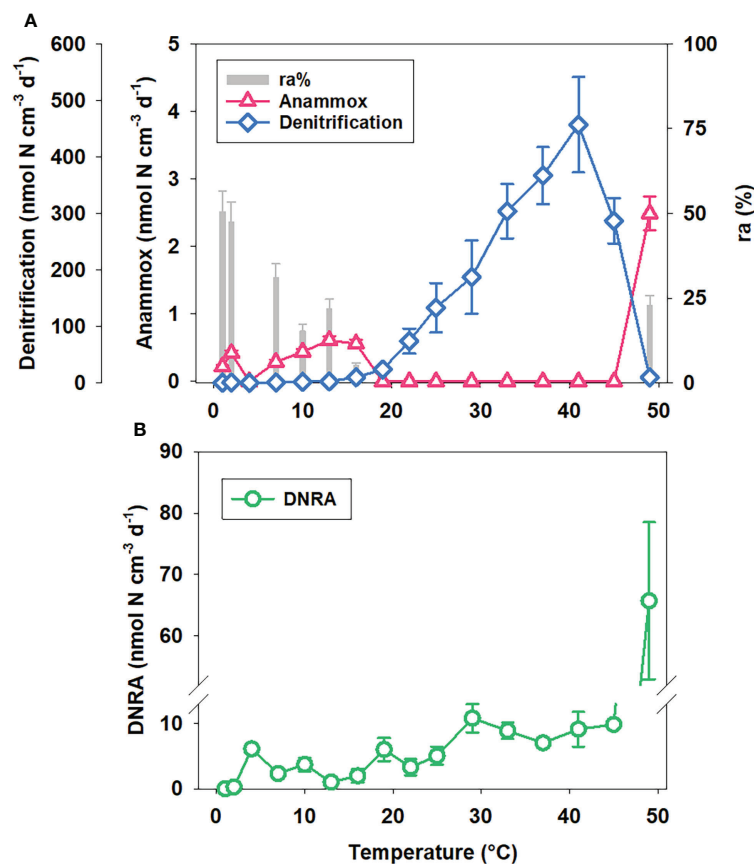


FIGURE 7 (A) Potential N-loss processes rates and ra and (B) potential DNRA rates at station D6 under different temperatures.

ra of 52.8% at the station with the highest TOC content in sediment, we predict that anammox is not only a significant but also the predominant process of benthic N-loss in KE, similar to in the Ulleung Basin (Na et al., 2018), and the Atacama and the Kermadec trench (Thamdrup et al., 2021).

On the other hand, meager denitrification (all under the detection limit) in  $^{15}\text{N}$  slurry incubation under *in situ* temperature can partly support the point that anammox is the predominant N-loss process in KE sediment as well. Denitrification is undetected mainly because of the high detection limit of  $^{30}\text{N}_2$  for membrane inlet mass spectrometer (MIMS) due to the interference of  $\text{NO}^+$ , whose molecular weight is also 30 produced in quadrupole mass spectrometer (An et al., 2001). Because ra calculated by flux or  $^{15}\text{N}$  slurry incubation is approximately the same (Engström et al., 2009; Rich et al., 2020; Thamdrup et al., 2021), we assume that ra is also 52.8% in sediment from Sta. D6 (5–7 cm), where anammox rate is the highest determined by  $^{15}\text{N}$  incubation. The highest denitrification rate estimated in this way is about  $0.22 \text{ nmol N cm}^{-3} \text{ (wet sediment) d}^{-1}$ , still far below the detection limit of our MIMS (about  $0.66 \text{ nmol N cm}^{-3} \text{ (wet sediment) d}^{-1}$  in our

home-made MIMS). It might remind us that MIMS is not likely suitable for determining denitrification with low activity in deep-ocean sediment.

### Temperature response of deep-ocean benthic dissimilatory nitrate reduction processes

Temperature affecting microbial enzyme activity is critical for dissimilatory nitrate reduction processes (Dalsgaard and Thamdrup, 2002; Brin et al., 2014). In the deep ocean with consistently low temperatures, present studies paid more attention to the effects of substrates like nitrate and organic carbon (Na et al., 2018; Rich et al., 2020), while the temperature responses were always selectively ignored. Our results of the temperature gradient  $^{15}\text{N}$  slurry incubation experiment in sediment with a water depth of over 5000 m precisely emphasize temperature as a crucial limiting factor for denitrification, anammox, and DNRA in deep ocean sediment. The lower  $T_{\text{opt}}$  (13°C) for anammox compared with

TABLE 4 Nitrification, denitrification, anammox rates, and ra reported from other deep-ocean sediment (water depth >1,000 m).

Location	Water depth (m)	Nitrification ( $\mu\text{mol N m}^{-2} \text{d}^{-1}$ )	Denitrification ( $\mu\text{mol N m}^{-2} \text{d}^{-1}$ )	Anammox ( $\mu\text{mol N m}^{-2} \text{d}^{-1}$ )	ra (%)	Reference
Porcupine Abyssal Plain	4,850	59 ± 26 <sup>a</sup>	5.1 ± 3.0 <sup>a</sup>	/	/	Brunnegård et al. (2004)
Washington margin	2,740–3,110	/	0–110 <sup>a</sup>	0–82 <sup>a</sup>	42 ± 5 <sup>a</sup>	Engström et al. (2009)
Sagami bay	1,450	/	37 ± 22 <sup>a</sup>	40 ± 18 <sup>a</sup>	52 ± 39 <sup>a</sup>	Glud et al. (2009)
		/	67 ± 25 <sup>b</sup>	/	36 ± 2 <sup>c</sup>	
North Atlantic slope	500–2,000	/	10 ± 3 <sup>b</sup>	15 ± 6 <sup>b</sup>	35–65 <sup>c</sup>	Trimmer and Nicholls (2009)
Arabian Sea	1,430	/	11 <sup>b</sup>	7 <sup>b</sup>	39 <sup>c</sup>	Sokoll et al. (2012)
Ulleung Basin	1,274–1,817 <sup>d</sup>	/	103 ± 41 <sup>b</sup>	63 ± 55 <sup>b</sup>	39 ± 11 <sup>c</sup>	Na et al. (2018)
	2,159–2,343 <sup>e</sup>	/	77 ± 10 <sup>b</sup>	101 ± 29 <sup>b</sup>	57 ± 5 <sup>c</sup>	
Peru margin	1,460–3,240	/	12–36 <sup>a</sup>	6–28 <sup>a</sup>	33–44 <sup>a</sup>	Rich et al. (2020)
Atacama trench	7,720–7,915	35 ± 15 <sup>a</sup>	3 ± 11 <sup>a</sup>	42 ± 16 <sup>a</sup>	67 ± 13 <sup>c</sup>	Thamdrup et al. (2021)
Kermadec trench	9,300–9,555	34 ± 8 <sup>a</sup>	2 ± 8 <sup>a</sup>	24 ± 12 <sup>a</sup>	91–98 <sup>c</sup>	Thamdrup et al. (2021)
Kuroshio Extension	5,548	6–42 <sup>a</sup>	14 <sup>a</sup>	16 <sup>a</sup>	53 <sup>a</sup>	This study

<sup>a</sup>Estimated from DIN fluxes.

<sup>b</sup>Estimated from <sup>15</sup>N intact core incubation.

<sup>c</sup>Estimated from <sup>15</sup>N slurry incubation.

<sup>d</sup>Stations at continental slope.

<sup>e</sup>Stations at basin.

denitrification confirms that marine anammox bacteria are psychrophile (Van De Vossenberg et al., 2008). It partly explains anammox as the dominant process for deep-ocean benthic N-loss in KE under low *in situ* temperature (~2°C). The activities of denitrification and DNRA can still increase significantly with temperature, indicating that temperature might be the primary limiting factor rather than substrates for denitrification and DNRA in northern KE with high pelagic primary production and organic matter supplement. The

maximum rates of anammox and DNRA at 49°C are most likely non-biological processes for few microorganisms could live under such a high temperature.

We summarize the results of temperature gradient experiments for N-loss processes reported from different marine sediments around the world in Table 5. The T<sub>opt</sub> (13°C) and Ea (54.5 ± 10.2 kJ mol<sup>-1</sup>) for anammox in our results are similar to marine sediment from high latitude areas where the temperature is constantly low (Dalsgaard and Thamdrup, 2002;

TABLE 5 Temperature gradient experiments for N-loss processes reported from other sediment (T<sub>ins</sub>, *in situ* temperature; T<sub>opt</sub>, optimal temperature; Ea, apparent activation energy).

Location	Water depth (m)	T <sub>ins</sub> (°C)	Denitrification		Anammox		Reference
			T <sub>opt</sub> (°C)	Ea (kJ mol <sup>-1</sup> )	T <sub>opt</sub> (°C)	Ea (kJ mol <sup>-1</sup> )	
Skagerrak	695	4–6	37	/	15	61	Dalsgaard and Thamdrup (2002)
Greenland coast	36–100	-1.7–4.0	24	60.6	12	51.0	Rysgaard et al. (2004)
Gulf of Mexico	1.5	29.9–31.8	35–37	102.7–123.5	/	/	Canion et al. (2014a)
Wadden Sea	0	19 <sup>c</sup>	26–35 <sup>c</sup>	51.7 ± 3.8 <sup>c</sup>	22–29 <sup>c</sup>	35.0 ± 4.9 <sup>c</sup>	Canion et al. (2014a)
		5.3 <sup>d</sup>	24–32 <sup>d</sup>	65.0 ± 4.0 <sup>d</sup>	/	/	
Svalbard	0	6.8	17–24	57.8 ± 4.4	9	/	Canion et al. (2014a)
Arctic fjord	51–210	-0.2–2.1	25–27	/	12–17	/	Canion et al. (2014b)
Rhode Island coast	38	6–7 <sup>a</sup>	22–35 <sup>a</sup>	43.7–60.4 <sup>a</sup>	25–33 <sup>a</sup>	34.3–38.2 <sup>a</sup>	Brin et al. (2017)
		11–17 <sup>b</sup>	18–31 <sup>b</sup>	38.5–50.5 <sup>b</sup>	21–31 <sup>b</sup>	38.0–66.9 <sup>b</sup>	
Providence River estuary	5	6 <sup>a</sup>	19–23 <sup>a</sup>	53.0 <sup>a</sup>	/	/	Brin et al. (2017)
		16–22 <sup>b</sup>	22–35 <sup>b</sup>	35.8–46.2 <sup>b</sup>	/	/	
Jiulong River estuary	0–11	30.0–36.5 <sup>c</sup>	>35 <sup>c</sup>	73.7 ± 9.8 <sup>c</sup>	25–30 <sup>c</sup>	41.2 ± 15.9 <sup>c</sup>	Tan et al. (2020)
		16.2–24.0 <sup>d</sup>	>30 <sup>d</sup>	74.0 ± 10.7 <sup>d</sup>	20–30 <sup>d</sup>	58.1 ± 10.4 <sup>d</sup>	
Kuroshio Extension	5,548	1.6	41	174.2 ± 9.6	13	54.5 ± 10.2	This study

<sup>a</sup>Sample was collected during January to March.

<sup>b</sup>Sample was collected during June to September.

<sup>c</sup>Sample was collected in summer.

<sup>d</sup>Sample was collected in winter.

Rysgaard et al., 2004; Canion et al., 2014a,  $T_{opt} = 9\text{--}17^\circ\text{C}$ ;  $E_a = 51\text{--}61 \text{ kJ mol}^{-1}$ ). However,  $T_{opt}$  for anammox is slightly lower than sediment from middle or low latitude areas, while  $E_a$  is generally higher (Canion et al., 2014a, b; Brin et al., 2017; Tan et al., 2020,  $T_{opt} = 20\text{--}33^\circ\text{C}$ ;  $E_a = 30.1\text{--}68.5 \text{ kJ mol}^{-1}$ ). This result suggests that anammox bacteria may adapt to higher and more variable temperatures. However,  $T_{opt}$  ( $41^\circ\text{C}$ ) and  $E_a$  ( $174.2 \pm 9.6 \text{ kJ mol}^{-1}$ ) for denitrification in our results are both surprisingly higher than in other areas ( $T_{opt} = 17\text{--}37^\circ\text{C}$   $E_a = 35.8\text{--}123.5 \text{ kJ mol}^{-1}$ ). This result emphasizes the much greater temperature dependence of heterotrophic denitrification bacteria in KE sediment with extremely low *in situ* temperature, explaining the low activity of benthic denitrification in the deep ocean from another perspective. Interestingly, the benthic denitrification bacteria community does not seem to show good adaptation to the low-temperature environment in the deep ocean of KE compared to the results on the Svalbard and Greenland coasts (Rysgaard et al., 2004; Canion et al., 2014a), but the reason for this result is still unclear.

Several studies have proved that DNRA can be enhanced with rising temperatures (King and Nedwell, 1984; Dong et al., 2011; Yin et al., 2017). Nevertheless, the results of the temperature gradient experiments reported were rare. The  $T_{opt}$  for DNRA in our results is hard to identify for the fluctuant increasing trend before  $29^\circ\text{C}$  (Figure 7B), while the temperature gradient incubation over  $30^\circ\text{C}$  has never been conducted before. Thus, the  $T_{opt}$  for DNRA is still uncertain. The  $E_a$  for DNRA in our results ( $91.9 \pm 22.9 \text{ kJ mol}^{-1}$ ) is comparable to the results reported in urban wetland sediments ( $50\text{--}107 \text{ kJ mol}^{-1}$ , Rahman et al., 2019) but much higher than the results in coastal sandy sediments ( $28 \text{ kJ mol}^{-1}$ , Kraft et al., 2014). The temperature dependence of DNRA is between denitrification and anammox in KE sediment ( $E_a$ : denitrification > DNRA > anammox). Our result is different from previous results, which indicated that the temperature dependence of denitrification was slightly lower than DNRA (Kraft et al., 2014; Rahman et al., 2019).

## Anammox and nitrification limited by ammonium

The concentration of substrates in pore-water is considered to be another significant factor for benthic N cycling processes (Dalsgaard et al., 2005). In continental margin sediment with high nitrate removal and ammonium production from mineralization activity, nitrate can be entirely depleted in the sediment at a few centimeters depth, and its concentration is usually below the half-saturation constant of nitrate ( $K_{m\_NO_3}$ ) for anammox ( $2.5 \mu\text{mol L}^{-1}$ , Lotti et al., 2014). While ammonium accumulates with depth, its concentration in the anoxic layer is generally much higher than  $K_{m\_NH_4}$  for anammox reported ( $<5 \mu\text{mol L}^{-1}$ , Strous et al., 1999). Thus, anammox is mainly limited by nitrate as the electron acceptor of the reaction in continental margin sediment (Gehring et al., 2010;

Song et al., 2013; Brin et al., 2014). However, in our results, the low concentration of ammonium in pore-water ( $<10 \mu\text{mol L}^{-1}$ ) and the discrepant anammox rates determined by anoxic incubation amended with  $^{15}\text{NO}_3^-$  and  $^{15}\text{NH}_4^+ + ^{14}\text{NO}_3^-$  ( $A_{P1}$  and  $A_{P2}$ ) both suggest that ammonium is the limiting substrate instead of nitrate for benthic anammox in the deep-ocean of KE (Figures 2B, 4B). The addition of ammonium in slurry incubations can significantly enhance anammox ( $A_{P2} > A_{P1}$ ), especially for the southern Sta. E10 and D2, which display entirely different characteristics compared to the result of continental margin sediments. The abnormally higher anammox rates detected in  $^{15}\text{NO}_3^-$  than in  $^{15}\text{NH}_4^+ + ^{14}\text{NO}_3^-$  amended incubation at Sta. D4 and E4 are possibly caused by overproduction of  $^{29}\text{N}_2$  via undetected denitrification. Despite similar pore-water ammonium profiles having been reported in deep margin and abyssal plain sediment (Christensen and Rowe, 1984; Berelson et al., 1990; Rich et al., 2020; Thamdrup et al., 2021), we first prove the significant influence of ammonium deficiency on anammox using  $^{15}\text{N}$  experimental methods. The excellent correlation between potential autotrophic anammox rates and TOC and TN also indicates that the mineralization of organic matter could be a crucial pathway of ammonium supplement under this condition (Figures 6D, E).

It is difficult to demonstrate whether nitrification is limited by ammonium in KE sediment like anammox using the  $^{15}\text{N}$  experiment for the excess addition of  $^{15}\text{NH}_4^+$  in the incubation system. Nevertheless, the comparison between total nitrification estimated from DIN fluxes ( $N_F$ ) and integrated potential nitrification rates ( $N_{IP}$ ), which respectively represent the genuine rates and potential nitrification activities in the oxic sediment zone, may provide some evidence (Figure 8). A similar comparison has been conducted in the Arabian Sea (Sokoll et al., 2012).  $N_{IP}$  is 1–2 orders of magnitude higher than  $N_F$  in our results, except for Sta. D4 and D6 ( $N_{IP}/N_F = 3.5$  and  $1.3$ , respectively), where sediment has a relatively abundant supplement of ammonium, indicating the possible existence of ammonium limitation for nitrification at other stations more or less. Moreover, an exponential decrease in the  $N_{IP}/N_F$  ratio may also indicate the growing effect of ammonium limitation from southern to northern stations (D2 to D6). It might be the reason why  $N_F$  has the highest value at the central Sta. D4, where potential nitrification activity and ammonium supplement are relatively high simultaneously. No significant correlation between potential rates of nitrification and either TOC, TN, or Chl-*a* might indicate that mineralization of organic matter might not be the only ammonium source. However, the ammonium limitation still exists for nitrification. We predict that the release of ammonium by microbes and meiofauna in the surface oxic sediment mentioned above could be another alternative ammonium source (Hall et al., 2007; Engström et al., 2009). Otherwise, the strong benthic  $\text{O}_2$  consumption could inhibit the growth of nitrification bacteria in the northern KE region (Ward, 2008), which could be the reason for the abnormally low nitrification rates in sediments with high TOC



and TN content (Figures 6A, B). Whereas more directly measured benthic nitrification rates in the deep ocean are required to verify the hypotheses above.

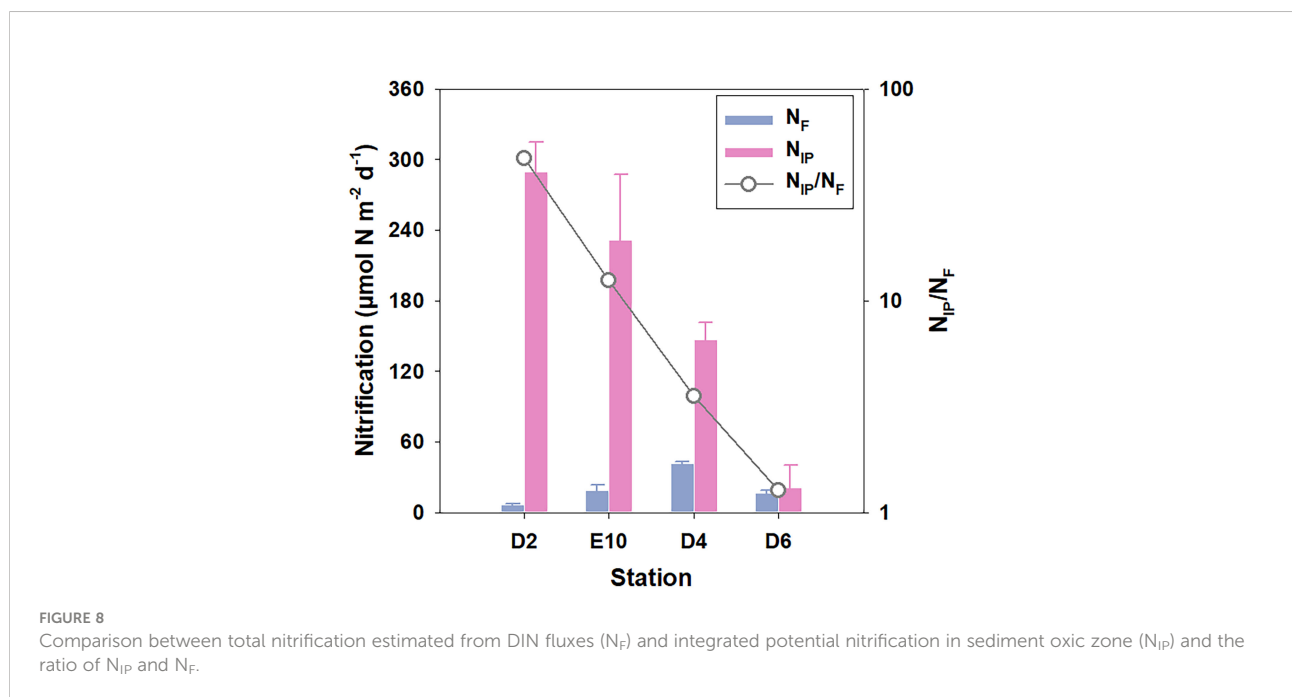
### Benthic nitrogen cycling regulated by pelagic primary production in KE

Organic matter plays a crucial role in benthic nitrogen cycling as both an energy source and an electron donor for heterotrophic denitrification, as well as a source of ammonium, which is the substrate for autotrophic anammox and nitrification (Devol, 2015). The organic matter in sediment is mainly derived from the transportation of biogenic elements like carbon *via* the biological pump, especially for the open ocean, with little effect from human activity (Lutz et al., 2007). Thus, as the first step of the biological pump, pelagic primary production, which transfers inorganic carbon into organic carbon, might also be a critical regulating factor for benthic nitrogen cycling.

Present studies based on satellite and underway observations demonstrate the high variability of NPP in KE (Lin et al., 2014; Clayton et al., 2021), agreeing well with the spatial distribution of total benthic N-loss in our results (Figure 1 and Table 3). In the northern KE (Sta. D6, which might include Sta. E4) with higher NPP, more abundant organic matter stimulates N-loss processes but limits nitrification because of the high O<sub>2</sub> consumption *via* the mineralization process. While in the southern KE (Sta. D4, E10, and D2), less organic matter supplemented, which makes autotrophic aerobic nitrification the predominant nitrogen cycling process. The sediment in KE generally shifts from nitrate sink to source from the north to the south with

decreased pelagic NPP (Table 3). Therefore, the pelagic primary production still significantly regulated the benthic N budget and the N cycling behaviors in KE with a water depth of over 5,000 m.

The limited data we obtained during this cruise makes it hard to deeply understand the nitrogen cycling processes in deep ocean sediments regulated by organic matter supplements. Therefore, we extracted the pore-water DIN data of the worldwide continental slope and abyssal plain sediments reported previously. The total nitrification and NO<sub>3</sub><sup>-</sup> loss rates were estimated using the method described in the present study (see *Materials and methods*). NO<sub>3</sub><sup>-</sup> loss rates (NO<sub>3</sub><sup>-</sup> to N<sub>2</sub> by denitrification and anammox) are used here to represent total N-loss activity because pore-water ammonium hardly accumulates with sediment depth, and the upward flux of ammonium cannot be obtained in abyssal plain sediments. The correlation between nitrification or NO<sub>3</sub><sup>-</sup> loss and water depth or NPP is shown in Figure 9. In abyssal plain areas, either benthic nitrification or NO<sub>3</sub><sup>-</sup> loss has a good correlation with NPP (Figures 9B, D, *p* < 0.001). However, the correlations between the two processes and water depth are relatively poor (Figures 9A, C, *p* = 0.046 and 0.064, respectively), unlike the traditional point claimed (Thamdrup and Dalsgaard, 2002; Dalsgaard et al., 2005; Na et al., 2018). It means pelagic primary production as the production step of the biological pump might play a more crucial role in organic matter supplementing the benthic N cycle in abyssal plain areas with relatively more minor depth variation (Figure 10). While in steep continental slope areas, nitrification or NO<sub>3</sub><sup>-</sup> loss shows a better correlation with water depth than NPP (Figure 9, *p* = 0.032 or < 0.001 for water depth and *p* = 0.063 or 0.083 for NPP, respectively). For the variation



of water depth is much more significant than the horizontal variation of NPP at different stations, the different decomposition levels of produced particulate organic matters during the vertical transportation and burial processes from the surface seawater to the seafloor might have more effect on the benthic N cycle (Figure 10). Our results highlight that benthic nitrogen cycling processes in abyssal plain areas are mainly regulated by pelagic primary production from the perspective of organic matter supplements, helping further understand the deep ocean benthic nitrogen cycle and the global nitrogen budget.

### Conclusions

In summary, our results demonstrate the spatial distribution and the limiting environmental factors of benthic nitrogen cycling processes (including nitrification and dissimilatory nitrate reduction) in the deep ocean of the Kuroshio Extension region. The N-loss rate decreases from north to south, while the nitrification rate is relatively higher in the central stations.

Anammox is considered to be the predominant N-loss process. The temperature gradient experiment indicates temperature as one of the limiting factors for benthic dissimilatory nitrate reduction processes. Compared to dominant psychrophilic anammox, denitrification with a surprisingly high optimal temperature and apparent activation energy is inhibited in consistently cold deep ocean sediment. Pore-water ammonium concentration is another limiting factor for anammox and nitrification in deep ocean sediment, unlike in margin sediment. The significant correlation between anammox and TOC, TN, and Chl-*a* indicates that mineralization of organic nitrogen is the primary ammonium source for anammox, while the supplement of ammonium might have other pathways for nitrification. Moreover, benthic N cycling is regulated by pelagic primary production, which produces organic matter and acts as both an energy source and a substrate source in the deep ocean. Overall, benthic N cycling in the deep ocean displays an entirely different feature from the marginal seas. Despite several relative studies that have led us to learn about the deep ocean benthic N cycling generally, however, actual measured data is severely lacking. Some fundamental

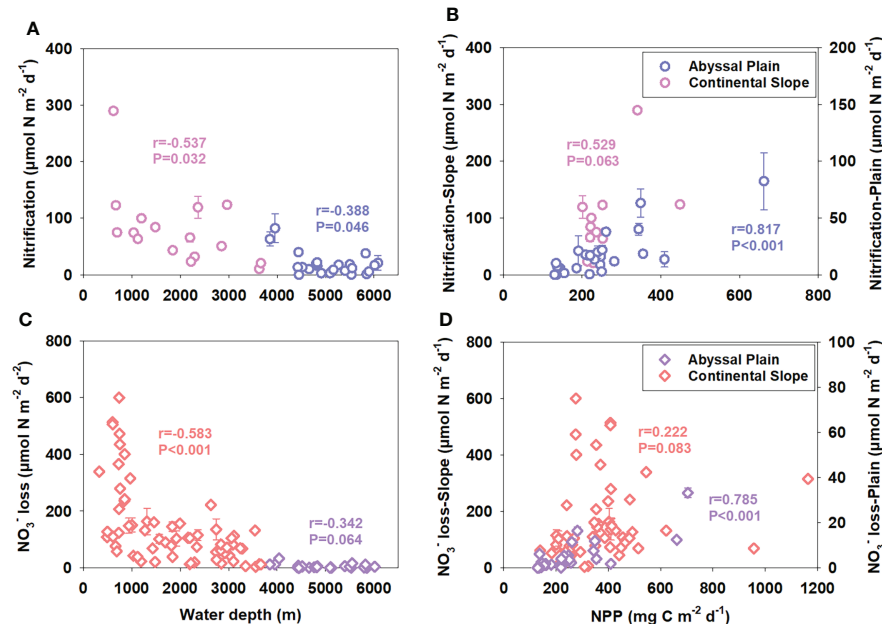


**FIGURE 9**  
Correlations between water depth (A, C) or pelagic net primary productivity (B, D) and benthic nitrification or NO<sub>3</sub><sup>-</sup> loss rates in worldwide abyssal plains and continental slopes. Stations with water depths over 3,800 m are considered to locate in abyssal plain areas. N cycling rates are estimated from published pore-water NO<sub>3</sub><sup>-</sup> profiles using the method described in this study (Emerson et al., 1980; Christensen and Rowe, 1984; De Lange, 1986; Sorensen et al., 1987; Nath and Mudholkar, 1989; Berelson et al., 1990; Balzer et al., 1998; Grandel et al., 2000; Hensen et al., 2000; Brunnegård et al., 2004; Engström et al., 2009; Jaeschke et al., 2010; Chong et al., 2012; Sokoll et al., 2012; Wankel et al., 2015; Rich et al., 2020; Thamdrup et al., 2021; This study) or are presented directly in the original article estimated via NO<sub>3</sub><sup>-</sup> fluxes obtained by a benthic lander (Jahnke and Jahnke, 2000) or measured using intact core incubation (Na et al., 2018). Pore-water NO<sub>3</sub><sup>-</sup> concentration not shown directly is extracted from the NO<sub>3</sub><sup>-</sup> profile images using WebPlotDigitizer (Version 4.5, <https://automeris.io/WebPlotDigitizer>).

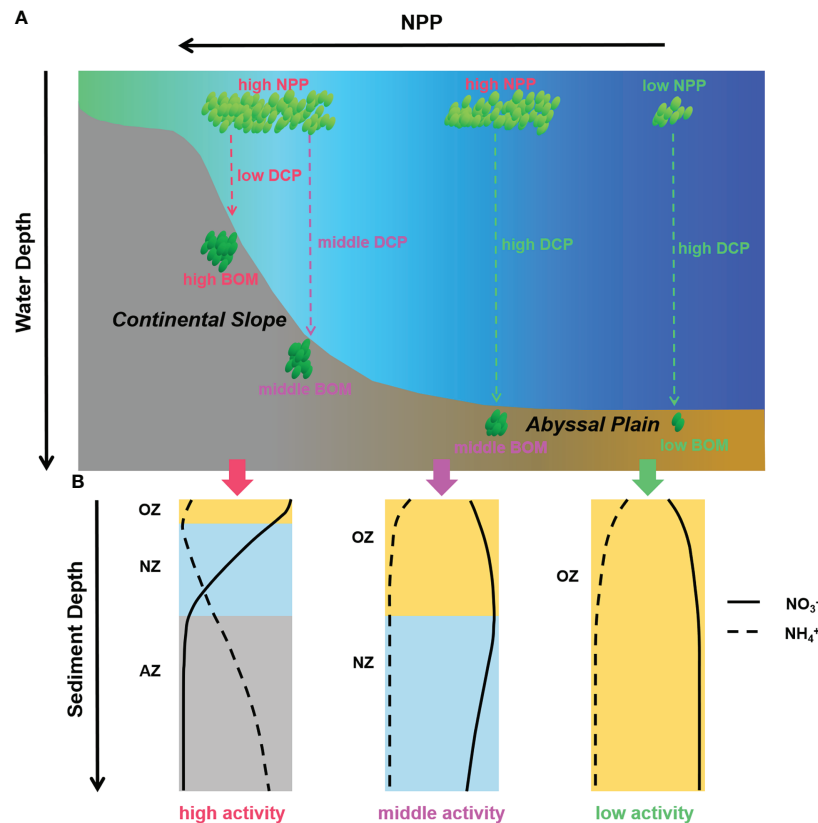


**FIGURE 10**  
**(A)** Production, transportation, and burial of organic matters in continental slope and abyssal plain areas and **(B)** different pore-water nitrate and ammonium profiles and benthic nitrogen cycling behaviors caused by various organic matter supplementation conditions. (NPP, net primary production; DCP, decomposition of organic matters; BOM, burial organic matters; OZ, oxic zone; NZ, anoxic nitrogenous zone; AZ, NO<sub>3</sub><sup>-</sup> depleted anoxic zone).

problems, such as the primary limiting factor of benthic N cycling processes in different deep ocean environments and their global implications, are still unclear and need more experimental evidence in the future.

manuscript. All authors contributed to the article and approved the submitted version.

### Data availability statement

The raw data supporting the conclusions of this article will be made available by the authors, without undue reservation.

### Funding

This study is financially supported by the National Science Foundation of China (U1806211, 42076035, and 41606093), the Fundamental Research Funds for the Central Universities (202072001), and the Taishan Scholars Programme of Shandong Province.

### Author contributions

GS and HX designed the study. HX performed the sampling procedures, onboard experiments and lab analyses with assistance from GS, SY and RZ. HX analyzed the data, wrote the manuscript and prepared the figures and tables. GS, GZ and SL provided comments on data analyses and revised the

### Acknowledgments

The captains and crew of *R/V Dongfanghong 3* are thanked for their help with field sampling. Guoling Zhang, Baichuan Wang, Peiyun Wu, and Haonan Wang are also acknowledged for their help in sample analysis and online NPP data acquisition. We sincerely thank two reviewers for the constructive comments.

This is MCTL (Key Laboratory of Marine Chemistry Theory and Technology) contribution #301.

## Conflict of interest

The authors declare that the research was conducted in the absence of any commercial or financial relationships that could be construed as a potential conflict of interest.

## References

- An, S., Gardner, W. S., and Kana, T. (2001). Simultaneous measurement of denitrification and nitrogen fixation using isotope pairing with membrane inlet mass spectrometry analysis. *Appl. Environ. Microbiol.* 67 (3), 1171–1178. doi: 10.1128/AEM.67.3.1171-1178.2001
- Balzer, W., Helder, W., Epping, E., Lohse, L., and Otto, S. (1998). Benthic denitrification and nitrogen cycling at the slope and rise of the NW European continental margin (Goban spur). *Prog. Oceanogr.* 42 (1-4), 111–126. doi: 10.1016/S0079-6611(98)00030-5
- Berelson, W. M., Hammond, D. E., O'neill, D., Xu, X. M., Chin, C., and Zuckin, J. (1990). Benthic fluxes and pore water studies from sediments of the central equatorial north pacific: Nutrient diagenesis. *Geochim. Cosmochim. Acta* 54 (11), 3001–3012. doi: 10.1016/0016-7037(90)90117-4
- Boudreau, B. P. (1997). *Diagenetic models and their implementation (Vol. 505)* (Berlin: Springer). doi: 10.1016/s0264-8172(98)80005-6
- Brin, L. D., Giblin, A. E., and Rich, J. J. (2014). Environmental controls of anammox and denitrification in southern new England estuarine and shelf sediments. *Limnol. Oceanogr.* 59 (3), 851–860. doi: 10.4319/lo.2014.59.3.0851
- Brin, L. D., Giblin, A. E., and Rich, J. J. (2017). Similar temperature responses suggest future climate warming will not alter partitioning between denitrification and anammox in temperate marine sediments. *Glob. Change Biol.* 23 (1), 331–340. doi: 10.1111/gcb.13370
- Brunnegård, J., Grandel, S., Ståhl, H., Tengberg, A., and Hall, P. O. (2004). Nitrogen cycling in deep-sea sediments of the porcupine abyssal plain, NE Atlantic. *Prog. Oceanogr.* 63 (4), 159–181. doi: 10.1016/j.pocan.2004.09.004
- Canfield, D. E., Glazer, A. N., and Falkowski, P. G. (2010). The evolution and future of earth's nitrogen cycle. *Science* 330 (6001), 192–196. doi: 10.1126/science.1186120
- Canion, A., Kostka, J. E., Gihring, T. M., Huettel, M., Van Beusekom, J. E. E., Gao, H., et al. (2014a). Temperature response of denitrification and anammox reveals the adaptation of microbial communities to *in situ* temperatures in permeable marine sediments that span 50 in latitude. *Biogeosciences* 11 (2), 309–320. doi: 10.5194/bg-11-309-2014
- Canion, A., Overholt, W. A., Kostka, J. E., Huettel, M., Lavik, G., and Kuypers, M. M. (2014b). Temperature response of denitrification and anaerobic ammonium oxidation rates and microbial community structure in Arctic fjord sediments. *Environ. Microbiol.* 16 (10), 3331–3344. doi: 10.1111/1462-2920.12593
- Chen, J. J., Erler, D. V., Wells, N. S., Huang, J., Welsh, D. T., and Eyre, B. D. (2021). Denitrification, anammox, and dissimilatory nitrate reduction to ammonium across a mosaic of estuarine benthic habitats. *Limnol. Oceanogr.* 66 (4), 1281–1297. doi: 10.1002/lno.11681
- Chong, L. S., Prokopenko, M. G., Berelson, W. M., Townsend-Small, A., and McManus, J. (2012). Nitrogen cycling within suboxic and anoxic sediments from the continental margin of Western north America. *Mar. Chem.* 128, 13–25. doi: 10.1016/j.marchem.2011.10.007
- Christensen, J. P., and Rowe, G. T. (1984). Nitrification and oxygen consumption in northwest Atlantic deep-sea sediments. *J. Mar. Res.* 42 (4), 1099–1116. doi: 10.1135/002224084788520828
- Clayton, S., Palevsky, H. I., Thompson, L., and Quay, P. D. (2021). Synoptic mesoscale to basin scale variability in biological productivity and chlorophyll in the kuroshio extension region. *J. Geophys. Res.-Oceans* 126 (11), e2021JC017782. doi: 10.1029/2021JC017782
- Dalsgaard, T., and Thamdrup, B. (2002). Factors controlling anaerobic ammonium oxidation with nitrite in marine sediments. *Appl. Environ. Microbiol.* 68 (8), 3802–3808. doi: 10.1128/AEM.68.8.3802-3808.2002
- Dalsgaard, T., Thamdrup, B., and Canfield, D. E. (2005). Anaerobic ammonium oxidation (anammox) in the marine environment. *Res. Microbiol.* 156 (4), 457–464. doi: 10.1016/j.resmic.2005.01.011
- De Lange, G. J. (1986). Early diagenetic reactions in interbedded pelagic and turbiditic sediments in the nares abyssal plain (western north atlantic): Consequences for the composition of sediment and interstitial water. *Geochim. Cosmochim. Acta* 50 (12), 2543–2561. doi: 10.1016/0016-7037(86)90209-7
- Devol, A. H. (2015). Denitrification, anammox, and N<sub>2</sub> production in marine sediments. *Annu. Rev. Mar. Sci.* 7, 403–423. doi: 10.1146/annurev-marine-010213-135040
- Dong, L. F., Sobey, M. N., Smith, C. J., Rusmana, I., Phillips, W., Stott, A., et al. (2011). Dissimilatory reduction of nitrate to ammonium, not denitrification or anammox, dominates benthic nitrate reduction in tropical estuaries. *Limnol. Oceanogr.* 56 (1), 279–291. doi: 10.4319/lo.2011.56.1.0279
- Emerson, S., Jahnke, R., Bender, M., Froelich, P., Klinkhammer, G., Bowser, C., et al. (1980). Early diagenesis in sediments from the eastern equatorial pacific, i. pore water nutrient and carbonate results. *Earth Planet. Sci. Lett.* 49 (1), 57–80. doi: 10.1016/0012-821X(80)90150-8
- Engström, P., Penton, C. R., and Devola, A. H. (2009). Anaerobic ammonium oxidation in deep-sea sediments off the Washington margin. *Limnol. Oceanogr.* 54 (5), 1643–1652. doi: 10.4319/lo.2009.54.5.1643
- Gihring, T. M., Lavik, G., Kuypers, M. M., and Kostka, J. E. (2010). Direct determination of nitrogen cycling rates and pathways in Arctic fjord sediments (Svalbard, Norway). *Limnol. Oceanogr.* 55 (2), 740–752. doi: 10.4319/lo.2010.55.2.0740
- Glud, R. N., Berg, P., Thamdrup, B., Larsen, M., Stewart, H. A., Jamieson, A. J., et al. (2021). Hadal trenches are dynamic hotspots for early diagenesis in the deep sea. *Commun. Earth Environ.* 2 (1), 1–8. doi: 10.1038/s43247-020-00087-2
- Glud, R. N., Thamdrup, B., Stahl, H., Wenzhoefer, F., Glud, A., Nomaki, H., et al. (2009). Nitrogen cycling in a deep ocean margin sediment (Sagami bay, Japan). *Limnol. Oceanogr.* 54 (3), 723–734. doi: 10.4319/lo.2009.54.3.0723
- Grandel, S., Rickert, D., Schlüter, M., and Wallmann, K. (2000). Pore-water distribution and quantification of diffusive benthic fluxes of silicic acid, nitrate and phosphate in surface sediments of the deep Arabian Sea. *Deep-Sea Res. Part II-Top. Stud. Oceanogr.* 47 (14), 2707–2734. doi: 10.1016/S0967-0645(00)00046-1
- Granger, J., and Sigman, D. M. (2009). Removal of nitrite with sulfamic acid for nitrate n and O isotope analysis with the denitrifier method. *Rapid Commun. Mass Spectrom.* 23 (23), 3753–3762. doi: 10.1002/rcm.4307
- Gruber, N., and Galloway, J. N. (2008). An earth-system perspective of the global nitrogen cycle. *Nature* 451, 293–296. doi: 10.1038/nature06592
- Hall, P. O., Brunnegård, J., Hulthe, G., Martin, W. R., Stahl, H., and Tengberg, A. (2007). Dissolved organic matter in abyssal sediments: Core recovery artifacts. *Limnol. Oceanogr.* 52 (1), 19–31. doi: 10.4319/lo.2007.52.1.0019
- Hansen, J. W., Thamdrup, B., and Jørgensen, B. B. (2000). Anoxic incubation of sediment in gas-tight plastic bags: A method for biogeochemical process studies. *Mar. Ecol.-Prog. Ser.* 208, 273–282. doi: 10.3354/meps208273
- Hensen, C., Zabel, M., and Schulz, H. D. (2000). A comparison of benthic nutrient fluxes from deep-sea sediments off Namibia and Argentina. *Deep-Sea Res. Part II-Top. Stud. Oceanogr.* 47 (9-11), 2029–2050. doi: 10.1016/S0967-0645(00)00015-1
- Holmes, R. M., Aminot, A., Kérouel, R., Hooker, B. A., and Peterson, B. J. (1999). A simple and precise method for measuring ammonium in marine and freshwater ecosystems. *Can. J. Fish. Aquat. Sci.* 56 (10), 1801–1808. doi: 10.1139/f99-128
- Howarth, R. W., and Marino, R. (2006). Nitrogen as the limiting nutrient for eutrophication in coastal marine ecosystems: Evolving views over three decades. *Limnol. Oceanogr.* 51 (1part2), 364–376. doi: 10.4319/lo.2006.51.1\_part\_2.0364

## Publisher's note

All claims expressed in this article are solely those of the authors and do not necessarily represent those of their affiliated organizations, or those of the publisher, the editors and the reviewers. Any product that may be evaluated in this article, or claim that may be made by its manufacturer, is not guaranteed or endorsed by the publisher.

- Hutchins, D. A., and Capone, D. G. (2022). The marine nitrogen cycle: New developments and global change. *Nat. Rev. Microbiol.* 20, 401–414. doi: 10.1038/s41579-022-00687-z
- Jaeschke, A., Abbas, B., Zabel, M., Hopmans, E. C., Schouten, S., and Sinninghe Damsté, J. S. (2010). Molecular evidence for anaerobic ammonium-oxidizing (anammox) bacteria in continental shelf and slope sediments off northwest Africa. *Limnol. Oceanogr.* 55 (1), 365–376. doi: 10.4319/lo.2010.55.1.0365
- Jahnke, R. A., and Jahnke, D. B. (2000). Rates of c, n, p and Si recycling and denitrification at the US mid-Atlantic continental slope depocenter. *Deep-Sea Res. Part I-Oceanogr. Res. Pap.* 47 (8), 1405–1428. doi: 10.1016/S0967-0637(99)00118-1
- Jamieson, A. J., and Stewart, H. A. (2021). Hadal zones of the northwest Pacific ocean. *Prog. Oceanogr.* 190, 102477. doi: 10.1016/j.pcean.2020.102477
- Kana, T. M., Darkangelo, C., Hunt, M. D., Oldham, J. B., Bennett, G. E., and Cornwell, J. C. (1994). Membrane inlet mass spectrometer for rapid high-precision determination of N<sub>2</sub>, O<sub>2</sub>, and ar in environmental water samples. *Anal. Chem.* 66 (23), 4166–4170. doi: 10.1021/ac00095a009
- King, D., and Nedwell, D. B. (1984). Changes in the nitrate-reducing community of an anaerobic saltmarsh sediment in response to seasonal selection by temperature. *Microbiology* 130 (11), 2935–2941. doi: 10.1099/00221287-130-11-2935
- Kraft, B., Tegetmeyer, H. E., Sharma, R., Klotz, M. G., Ferdelman, T. G., Hettich, R. L., et al. (2014). The environmental controls that govern the end product of bacterial nitrate respiration. *Science* 345 (6197), 676–679. doi: 10.1126/science.1254070
- Kuypers, M. M., Marchant, H. K., and Kartal, B. (2018). The microbial nitrogen-cycling network. *Nat. Rev. Microbiol.* 16 (5), 263–276. doi: 10.1038/nrmicro.2018.9
- Li, Y., and Gregory, S. (1974). Diffusion of ions in sea water and in deep-sea sediments. *Geochim. Cosmochim. Acta* 38 (5), 703–714. doi: 10.1016/0016-7037(74)90145-8
- Lin, P., Chai, F., Xue, H., and Xiu, P. (2014). Modulation of decadal oscillation on surface chlorophyll in the kuroshio extension. *J. Geophys. Res.-Oceans* 119 (1), 187–199. doi: 10.1002/2013JC009359
- Lotti, T., Kleerebezem, R., Lubello, C., and Van Loosdrecht, M. C. M. (2014). Physiological and kinetic characterization of a suspended cell anammox culture. *Water Res.* 60, 1–14. doi: 10.1016/j.watres.2014.04.017
- Lutz, M. J., Caldeira, K., Dunbar, R. B., and Behrenfeld, M. J. (2007). Seasonal rhythms of net primary production and particulate organic carbon flux to depth describe the efficiency of biological pump in the global ocean. *J. Geophys. Res.-Oceans* 112, C10011. doi: 10.1029/2006JC003706
- Middelburg, J. J., Soetaert, K., Herman, P. M., and Heip, C. H. (1996). Denitrification in marine sediments: A model study. *Glob. Biogeochem. Cycle* 10 (4), 661–673. doi: 10.1029/96GB02562
- Na, T., Thamdrup, B., Kim, B., Kim, S. H., Vandieken, V., Kang, D. J., et al. (2018). N<sub>2</sub> production through denitrification and anammox across the continental margin (shelf–slope–rise) of the ulleung basin, East Sea. *Limnol. Oceanogr.* 63 (S1), S410–S424. doi: 10.1002/lno.10750
- Nath, B. N., and Mudholkar, A. V. (1989). Early diagenetic processes affecting nutrients in the pore waters of central Indian ocean cores. *Mar. Geol.* 86 (1), 57–66. doi: 10.1016/0025-3227(89)90018-2
- Pinckney, J., Papa, R., and Zingmark, R. (1994). Comparison of high-performance liquid chromatographic, spectrophotometric, and fluorometric methods for determining chlorophyll *a* concentrations in estuarine sediments. *J. Microbiol. Methods* 19 (1), 59–66. doi: 10.1016/0167-7012(94)90026-4
- Rahman, M., Grace, M. R., Roberts, K. L., Kessler, A. J., and Cook, P. L. (2019). Effect of temperature and drying-rewetting of sediments on the partitioning between denitrification and DNRA in constructed urban stormwater wetlands. *Ecol. Eng.* 140, 105586. doi: 10.1016/j.ecoleng.2019.105586
- Rich, J. J., Arevalo, P., Chang, B. X., Devol, A. H., and Ward, B. B. (2020). Anaerobic ammonium oxidation (anammox) and denitrification in Peru margin sediments. *J. Mar. Syst.* 207, 103122. doi: 10.1016/j.jmarsys.2018.09.007
- Rysgaard, S., Glud, R. N., Risgaard-Petersen, N., and Dalsgaard, T. (2004). Denitrification and anammox activity in Arctic marine sediments. *Limnol. Oceanogr.* 49 (5), 1493–1502. doi: 10.4319/lo.2004.49.5.1493
- Schnetger, B., and Lehnert, C. (2014). Determination of nitrate plus nitrite in small volume marine water samples using vanadium (III) chloride as a reduction agent. *Mar. Chem.* 160, 91–98. doi: 10.1016/j.marchem.2014.01.010
- Soetaert, K., Herman, P. M., and Middelburg, J. J. (1996). A model of early diagenetic processes from the shelf to abyssal depths. *Geochim. Cosmochim. Acta* 60 (6), 1019–1040. doi: 10.1016/0016-7037(96)00013-0
- Sokoll, S., Holtappels, M., Lam, P., Collins, G., Schlüter, M., Lavik, G., et al. (2012). Benthic nitrogen loss in the Arabian Sea off Pakistan. *Front. Microbiol.* 3. doi: 10.3389/fmicb.2012.00395
- Song, G. D., Liu, S. M., Marchant, H., Kuypers, M. M., and Lavik, G. (2013). anammox, denitrification and dissimilatory nitrate reduction to ammonium in the East China Sea sediment. *Biogeosciences* 10 (11), 6851–6864. doi: 10.5194/bg-10-6851-2013
- Sorensen, J., Jorgensen, K. S., Colley, S., Hydes, D. J., Thomson, J., and Wilson, T. R. S. (1987). Depth localization of denitrification in a deep-sea sediment from the Madeira abyssal plain I. *Limnol. Oceanogr.* 32 (3), 758–762. doi: 10.4319/lo.1987.32.3.0758
- Strous, M., Kuenen, J. G., and Jetten, M. S. (1999). Key physiology of anaerobic ammonium oxidation. *Appl. Environ. Microbiol.* 65 (7), 3248–3250. doi: 10.1128/AEM.65.7.3248-3250.1999
- Tan, E., Zou, W., Zheng, Z., Yan, X., Du, M., Hsu, T. C., et al. (2020). Warming stimulates sediment denitrification at the expense of anaerobic ammonium oxidation. *Nat. Clim. Change* 10 (4), 349–355. doi: 10.1038/s41558-020-0723-2
- Thamdrup, B., and Dalsgaard, T. (2000). The fate of ammonium in anoxic manganese oxide-rich marine sediment. *Geochim. Cosmochim. Acta* 64 (24), 4157–4164. doi: 10.1016/S0016-7037(00)00496-8
- Thamdrup, B., and Dalsgaard, T. (2002). Production of N<sub>2</sub> through anaerobic ammonium oxidation coupled to nitrate reduction in marine sediments. *Appl. Environ. Microbiol.* 68 (3), 1312–1318. doi: 10.1128/AEM.68.3.1312-1318.2002
- Thamdrup, B. O., and Dalsgaard, T. (2008). “Nitrogen cycling in sediments,” in *Microbial Ecology of the Oceans*, ed. D. L. Kirchman (Hoboken, NJ: John Wiley & Sons, Inc.), 527–567. doi: 10.1002/9780470281840.ch14
- Thamdrup, B., Schauberger, C., Larsen, M., Trouche, B., Maignien, L., Arnaud-Haond, S., et al. (2021). Anammox bacteria drive fixed nitrogen loss in hadal trench sediments. *Proc. Natl. Acad. Sci. U. S. A.* 118 (46), e2104529118. doi: 10.1073/pnas.2104529118
- Tiedje, J. M. (1988). Ecology of denitrification and dissimilatory nitrate reduction to ammonium,” in *Environmental Microbiology of Anaerobes*, ed. A. J. B. Zehnder, (New York, NY: John Wiley & Sons), 179–244. doi: 10.1016/b978-0-12-160280-2.50014-6
- Trimmer, M., and Nicholls, J. C. (2009). Production of nitrogen gas via anammox and denitrification in intact sediment cores along a continental shelf to slope transect in the north Atlantic. *Limnol. Oceanogr.* 54 (2), 577–589. doi: 10.4319/lo.2009.54.2.0577
- Uchiyama, Y., Suzue, Y., and Yamazaki, H. (2017). Eddy-driven nutrient transport and associated upper-ocean primary production along the kuroshio. *J. Geophys. Res.-Oceans* 122 (6), 5046–5062. doi: 10.1002/2017JC012847
- Van De Vossenberg, J., Rattray, J. E., Geerts, W., Kartal, B., Van Niftrik, L., Van Donselaar, E. G., et al. (2008). Enrichment and characterization of marine anammox bacteria associated with global nitrogen gas production. *Environ. Microbiol.* 10 (11), 3120–3129. doi: 10.1111/j.1462-2920.2008.01643.x
- Wankel, S. D., Buchwald, C., Ziebis, W., Wenk, C. B., and Lehmann, M. F. (2015). Nitrogen cycling in the deep sedimentary biosphere: Nitrate isotopes in porewaters underlying the oligotrophic north Atlantic. *Biogeosciences* 12 (24), 7483–7502. doi: 10.5194/bg-12-7483-2015
- Ward, B. B. (2008). “Nitrification in marine systems,” in *Nitrogen in the marine environment, 2nd Edition* (San Diego: Academic Press, Elsevier), 199–261.
- WebPlotDigitizer. (2022). WebPlotDigitizer (Version 4.5). Available at: <https://automeris.io/WebPlotDigitizer> (Accessed July 12, 2022).
- Yin, G., Hou, L., Liu, M., Liu, Z., and Gardner, W. S. (2014). A novel membrane inlet mass spectrometer method to measure <sup>15</sup>NH<sub>4</sub><sup>+</sup> for isotope-enrichment experiments in aquatic ecosystems. *Environ. Sci. Technol.* 48 (16), 9555–9562. doi: 10.1021/es501261s
- Yin, G., Hou, L., Liu, M., Li, X., Zheng, Y., Gao, J., et al. (2017). DNRA in intertidal sediments of the Yangtze estuary. *J. Geophys. Res.-Biogeosci.* 122 (8), 1988–1998. doi: 10.1002/2017JG003766